

Characterizing and Adapting the Consistency-Latency Tradeoff in Distributed Key-value Stores

MUNTASIR RAIHAN RAHMAN, LEWIS TSENG, SON NGUYEN, INDRANIL GUPTA,
NITIN VAIDYA, University of Illinois at Urbana-Champaign

The CAP theorem is a fundamental result that applies to distributed storage systems. In this paper, we first present and prove two CAP-like impossibility theorems. To state these theorems, we present probabilistic models to characterize the three important elements of the CAP theorem: consistency (C), availability or latency (A), and partition tolerance (P). The theorems show the un-achievable envelope, i.e., which combinations of the parameters of the three models make them impossible to achieve together. Next, we present the design of a class of systems called PCAP that perform close to the envelope described by our theorems. In addition, these systems allow applications running on a single data-center to specify either a latency SLA or a consistency SLA. The PCAP systems automatically adapt, in real-time and under changing network conditions, to meet the SLA while optimizing the other C/A metric. We incorporate PCAP into two popular key-value stores – Apache Cassandra and Riak. Our experiments with these two deployments, under realistic workloads, reveal that the PCAP systems satisfactorily meets SLAs, and perform close to the achievable envelope. We also extend PCAP from a single data-center to multiple geo-distributed data-centers.

CCS Concepts: • **Information systems** → **Distributed storage**;

Additional Key Words and Phrases: Consistency, Adaptivity, Distributed Storage

1. INTRODUCTION

Storage systems form the foundational platform for modern Internet services such as Web search, analytics, and social networking. Ever increasing user bases and massive data sets have forced users and applications to forgo conventional relational databases, and move towards a new class of scalable storage systems known as NoSQL key-value stores. Many of these distributed key-value stores (e.g., Cassandra [Lakshman and Malik 2008], Riak [Gross 2009], Dynamo [DeCandia et al. 2007], Voldemort [LinkedIn 2009]) support a simple GET/PUT interface for accessing and updating data items. The data items are replicated at multiple servers for fault tolerance. In addition, they offer a very weak notion of consistency known as eventual consistency [Vogels 2009; Bailis and Ghodsi 2013], which roughly speaking, says that if no further updates are sent to a given data item, all replicas will eventually hold the same value.

These key-value stores are preferred by applications for whom eventual consistency suffices, but where high availability and low latency (i.e., fast reads and writes [Abadi 2012]) are paramount. Latency is a critical metric for such cloud services because latency is correlated to user satisfaction – for instance, a 500 ms increase in latency for operations at Google.com can cause a 20% drop in revenue [Peled 2010]. At Amazon, this translates to a \$6M yearly loss per added millisecond of latency [Lang 2009]. This correlation between delay and lost retention is fundamentally human. Humans suffer from a phenomenon called *user cognitive drift*, wherein if more than a second (or so) elapses between clicking on something and receiving a response, the user’s mind is already elsewhere.

This work was supported in part by the following grants: NSF CNS 1409416, NSF CNS 1319527, NSF CCF 0964471, AFOSR/AFRL FA8750-11-2-0084, VMware Graduate Fellowship, Yahoo!, and a generous gift from Microsoft.

Author’s addresses: M. Rahman, L. Tseng, S. Nguyen, I. Gupta, Department of Computer Science; N. Vaidya, Department of Electrical and Computer Engineering, University of Illinois at Urbana-Champaign (UIUC).

Permission to make digital or hard copies of all or part of this work for personal or classroom use is granted without fee provided that copies are not made or distributed for profit or commercial advantage and that copies bear this notice and the full citation on the first page. Copyrights for components of this work owned by others than ACM must be honored. Abstracting with credit is permitted. To copy otherwise, or republish, to post on servers or to redistribute to lists, requires prior specific permission and/or a fee. Request permissions from permissions@acm.org.

© 2016 ACM. 1556-4665/2016/09-ARTXXXX \$15.00

DOI : <http://dx.doi.org/10.1145/0000000.0000000>

At the same time, clients in such applications expect freshness, i.e., data returned by a read to a key should come from the latest writes done to that key by any client. For instance, Netflix uses Cassandra to track positions in each video [Cockcroft 2013], and freshness of data translates to accurate tracking and user satisfaction. This implies that clients care about a *time-based* notion of data freshness. Thus, this paper focuses on consistency based on the notion of data freshness (as defined later).

The CAP theorem was proposed by Eric Brewer [2000, 2010], and later formally proved by Gilbert and Lynch [2012, 2002]. It essentially states that a system can choose at most two of three desirable properties: Consistency (C), Availability (A), and Partition tolerance (P). Recently, Abadi [2012] proposed to study the consistency-latency tradeoff, and unified the tradeoff with the CAP theorem. The unified result is called PACELC. It states that when a network partition occurs, one needs to choose between Availability and Consistency; otherwise the choice is between Latency and Consistency. We focus on the latter tradeoff as it is the common case. These prior results provided qualitative characterization of the tradeoff between consistency and availability/latency, while we provide a *quantitative* characterization of the tradeoff.

Concretely, traditional CAP literature tends to focus on situations where “hard” network partitions occur and the designer has to choose between C or A, e.g., in geo-distributed data-centers. However, individual data-centers themselves suffer far more frequently from “soft” partitions [Dean 2009], arising from periods of elevated message delays or loss rates (i.e., the “otherwise” part of PACELC) within a data-center. Neither the original CAP theorem nor the existing work on consistency in key-value stores [Bailis et al. 2014; DeCandia et al. 2007; Glendenning et al. 2011; Wei et al. 2015; Li et al. 2012; Lloyd et al. 2011, 2013; Shapiro et al. 2011; Terry et al. 2013; Vogels 2009] address such soft partitions for a single data-center.

In this paper we state and prove two CAP-like impossibility theorems. To state these theorems, we present probabilistic¹ models to characterize the three important elements: soft partition, latency requirements, and consistency requirements. All our models take timeliness into account. Our latency model specifies soft bounds on operation latencies, as might be provided by the application in an SLA (Service Level Agreement). Our consistency model captures the notion of data freshness returned by read operations. Our partition model describes propagation delays in the underlying network. The resulting theorems show the un-achievable envelope, i.e., which combinations of the parameters in these three models (partition, latency, consistency) make them impossible to achieve together. Note that the focus of the paper is neither defining a new consistency model nor comparing different types of consistency models. Instead, we are interested in the un-achievable envelope of the three important elements and measuring how close a system can perform to this envelope.

Next, we describe the design of a class of systems called PCAP (short for Probabilistic CAP) that perform close to the envelope described by our theorems. In addition, these systems allow applications running inside a single data-center to specify either a probabilistic latency SLA or a probabilistic consistency SLA. Given a probabilistic latency SLA, PCAP’s adaptive techniques meet the specified operational latency requirement, while optimizing the consistency achieved. Similarly, given a probabilistic consistency SLA, PCAP meets the consistency requirement while optimizing operational latency. PCAP does so under real and continuously changing network conditions. There are known use cases that would benefit from an latency SLA – these include the Netflix video tracking application [Cockcroft 2013], online advertising [Barr 2013], and shopping cart applications [Terry et al. 2013] – each of these needs fast response times but is willing to tolerate some staleness. A known use case for consistency SLA is a Web search application [Terry et al. 2013], which desires search results with bounded staleness but would like to minimize the response time. While the PCAP system can be used with a variety of consistency and latency models (like PBS [Bailis et al. 2014]), we use our PCAP models for concreteness.

We have integrated our PCAP system into two key-value stores – Apache Cassandra [Lakshman and Malik 2008] and Riak [Gross 2009]. Our experiments with these two deployments, using

¹By probabilistic, we mean the behavior is statistical over a long time period.

YCSB [Cooper et al. 2010a] benchmarks, reveal that PCAP systems satisfactorily meets a latency SLA (or consistency SLA), optimize the consistency metric (respectively latency metric), perform reasonably close to the envelope described by our theorems, and scale well.

We also extend PCAP from a single data-center to multiple geo-distributed data-centers. The key contribution of our second system (which we call GeoPCAP) is a set of rules for composing probabilistic consistency/latency models from across multiple data-centers in order to derive the global consistency-latency tradeoff behavior. Realistic simulations demonstrate that GeoPCAP can satisfactorily meet consistency/latency SLAs for applications interacting with multiple data-centers, while optimizing the other metric.

2. CONSISTENCY-LATENCY TRADEOFF

We consider a key-value store system which provides a read/write API over an asynchronous distributed message-passing network. The system consists of clients and servers, in which, servers are responsible for replicating the data (or read/write object) and ensuring the specified consistency requirements, and clients can invoke a write (or read) operation that stores (or retrieves) some value of the specified key by contacting server(s). We assume each client has a corresponding client proxy at the set of servers, which submits read and write operations on behalf of clients [Lloyd et al. 2011; Shapiro 1986]. Specifically, in the system, data can be propagated from a writer client to multiple servers by a replication mechanism or background mechanism such as read repair [DeCandia et al. 2007], and the data stored at servers can later be read by clients. There may be multiple versions of the data corresponding to the same key, and the exact value to be read by reader clients depends on how the system ensures the consistency requirements. Note that as addressed earlier, we define consistency based on freshness of the value returned by read operations (defined below). We first present our probabilistic models for soft partition, latency and consistency. Then we present our impossibility results. These results only hold for a single data-center. Later in Section 4 we deal with the multiple data-center case.

2.1. Models

To capture consistency, we defined a new notion called *t-freshness*, which is a form of eventual consistency. Consider a single key (or read/write object) being read and written concurrently by multiple clients. An operation O (read or write) has a start time $\tau_{start}(O)$ when the client issues O , and a finish time $\tau_{finish}(O)$ when the client receives an answer (for a read) or an acknowledgment (for a write). The write operation ends when the client receives an acknowledgment from the server. The value of a write operation can be reflected on the server side (i.e., visible to other clients) any time after the write starts. For clarity of our presentation, we assume that all write operations end in this paper, which is reasonable given client retries. Note that the written value can still propagate to other servers after the write ends by the background mechanism. We assume that at time 0 (initial time), the key has a default value.

Definition 2.1. t-freshness and t-staleness: A read operation R is said to be *t-fresh* if and only if R returns a value written by any write operation that starts at or after time $\tau_{fresh}(R, t)$, which is defined below:

- (1) If there is at least one write starting in the interval $[\tau_{start}(R) - t, \tau_{start}(R)]$: then $\tau_{fresh}(R, t) = \tau_{start}(R) - t$.
- (2) If there is no write starting in the interval $[\tau_{start}(R) - t, \tau_{start}(R)]$, then there are two cases:
 - (a) No write starts before R starts: then $\tau_{fresh}(R, t) = 0$.
 - (b) Some write starts before R starts: then $\tau_{fresh}(R, t)$ is the start time of the last write operation that starts before $\tau_{start}(R) - t$.

A read that is not *t-fresh* is said to be *t-stale*.

Note that the above characterization of $\tau_{fresh}(R, t)$ only depends on *start times* of operations.

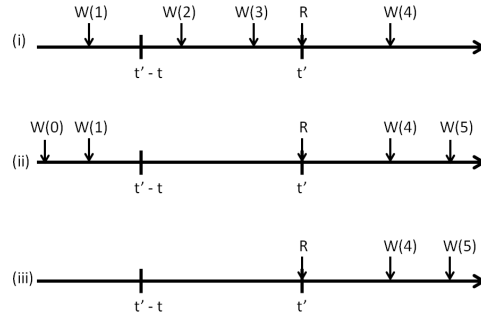


Fig. 1. Examples illustrating Definition 2.1. Only start times of each operation are shown.

Fig. 1 shows three examples for t -freshness. The figure shows the times at which several read and write operations are issued (the time when operations complete are not shown in the figure). $W(x)$ in the figure denotes a write operation with a value x . Note that our definition of t -freshness allows a read to return a value that is written by a write issued after the read is issued. In Fig. 1(i), $\tau_{fresh}(R, t) = \tau_{start}(R) - t = t' - t$; therefore, R is t -fresh if it returns 2, 3 or 4. In Fig. 1(ii), $\tau_{fresh}(R, t) = \tau_{start}(W(1))$; therefore, R is t -fresh if it returns 1, 4 or 5. In Fig. 1(iii), $\tau_{fresh}(R, t) = 0$; therefore, R is t -fresh if it returns 4, 5 or the default.

Definition 2.2. Probabilistic Consistency: A key-value store satisfies (t_c, p_{ic}) -consistency² if in any execution of the system, the fraction of read operations satisfying t_c -freshness is at least $(1 - p_{ic})$.

Intuitively, p_{ic} is the *likelihood of returning stale data*, given the time-based freshness requirement t_c .

Two similar definitions have been proposed previously: (1) t -visibility from the Probabilistically Bounded Staleness (PBS) work [Bailis et al. 2014], and (2) Δ -atomicity [Golab et al. 2011]. These two metrics do not require a read to return the latest write, but provide a time bound on the staleness of the data returned by the read. The main difference between t -freshness and these is that we consider the start time of write operations rather than the end time. This allows us to characterize consistency-latency tradeoff more precisely. While we prefer t -freshness, our PCAP system (Section 3) is modular and could use instead t -visibility or Δ -atomicity for estimating data freshness.

As noted earlier, our focus is not comparing different consistency models, nor achieving linearizability. We are interested in the un-achievable envelope of soft partition, latency requirements, and consistency requirements. Traditional consistency models like linearizability can be achieved by delaying the effect of a write. On the contrary, the achievability of t -freshness closely ties to the latency of read operations and underlying network behavior as discussed later. In other words, t -freshness by itself is not a complete definition.

2.1.1. Use case for t -freshness. Consider a bidding application (e.g., eBay), where everyone can post a bid, and we want every other participant to see posted bids as fast as possible. Assume that User 1 submits a bid, which is implemented as a write request (Figure 2). User 2 requests to read the bid before the bid write process finishes. The same User 2 then waits a finite amount of time after the bid write completes and submits another read request. Both of these read operations must reflect User 1's bid, whereas t -visibility only reflects the write in User 2's second read (with suitable choice of t). The bid write request duration can include time to send back an acknowledgment to

²The subscripts c and ic stand for consistency and inconsistency, respectively.

the client, even after the bid has committed (on the servers). A client may not want to wait that long to see a submitted bid. This is especially true when the auction is near the end.

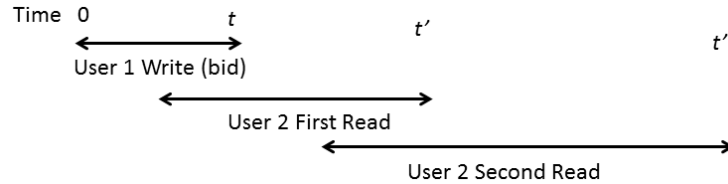


Fig. 2. Example motivating use of Definition 2.2.

We define our probabilistic notion of latency as follows:

Definition 2.3. t -latency: A read operation R is said to satisfy t -latency if and only if it completes within t time units of its start time.

Definition 2.4. Probabilistic Latency: A key-value store satisfies (t_a, p_{ua}) -latency³ if in any execution of the system, the fraction of t_a -latency read operations is at least $(1 - p_{ua})$.

Intuitively, given response time requirement t_a ,
 p_{ua} is the likelihood of a read violating the t_a .

Finally, we capture the concept of a *soft partition* of the network by defining a probabilistic partition model. In this section, we assume that the partition model for the network does not change over time. (Later, our implementation and experiments in Section 5 will measure the effect of time-varying partition models.)

In a key-value store, data can propagate from one client to another via the other servers using different approaches. For instance, in Apache Cassandra [Lakshman and Malik 2008], a write might go from a writer client to a coordinator server to a replica server, or from a replica server to another replica server in the form of read repair [DeCandia et al. 2007]. Our partition model captures the delay of all such propagation approaches. Please note that the partition model applies not to the network directly, but to the paths taken by the read or write operation queries themselves. This means that the network as a whole may be good (or bad), but if the paths taken by the queries are bad (or good), only the latter matters.

Definition 2.5. Probabilistic Partition:

An execution is said to suffer (t_p, α) -partition if the fraction f of paths from one client to another client, via a server, which have latency higher than t_p , is such that $f \geq \alpha$.

Our delay model loosely describes the message delay caused by any underlying network behavior without relying on the assumptions on the implementation of the key-value store. We do not assume eventual delivery of messages. We neither define propagation delay for each message nor specify the propagation paths (or alternatively, the replication mechanisms). This is because we want to have general lower bounds that apply to all systems that satisfy our models.

³The subscripts a and ua stand for availability and unavailability, respectively.

2.2. Impossibility Results

We now present two theorems that characterize the consistency-latency tradeoff in terms of our probabilistic models.

First, we consider the case when the client has tight expectations, i.e., the client expects all data to be fresh within a time bound, and all reads need to be answered within a time bound.

THEOREM 2.6. *If $t_c + t_a < t_p$, then it is impossible to implement a read/write data object under a $(t_p, 0)$ -partition while achieving $(t_c, 0)$ -consistency, and $(t_a, 0)$ -latency, i.e., there exists an execution such that these three properties cannot be satisfied simultaneously.*

PROOF. The proof is by contradiction. In a system that satisfies all three properties in all executions, consider an execution with only two clients, a writer client and a reader client. There are two operations: (i) the writer client issues a write W , and (ii) the reader client issues a read R at time $\tau_{start}(R) = \tau_{start}(W) + t_c$. Due to $(t_c, 0)$ -consistency, the read R must return the value from W .

Let the delay of the write request W be exactly t_p units of time (this obeys $(t_p, 0)$ -partition). Thus, the earliest time that W 's value can arrive at the reader client is $(\tau_{start}(W) + t_p)$. However, to satisfy $(t_a, 0)$ -latency, the reader client must receive an answer by time $\tau_{start}(R) + t_a = \tau_{start}(W) + t_c + t_a$. However, this time is earlier than $(\tau_{start}(W) + t_p)$ because $t_c + t_a < t_p$. Hence, the value returned by W cannot satisfy $(t_c, 0)$ -consistency. This is a contradiction. \square

Essentially, the above theorem relates the clients' expectations of freshness (t_c) and latency (t_a) to the propagation delays (t_p). If client expectations are too stringent when the maximum propagation delay is large, then it may not be possible to guarantee both consistency and latency expectations.

However, if we allow a fraction of the reads to return late (i.e., after t_a), or return t_c -stale values (i.e., when either p_{ic} or p_{ua} is non-zero), then it may be possible to satisfy the three properties together even if $t_c + t_a < t_p$. Hence, we consider non-zero p_{ic}, p_{ua} and α in our second theorem.

THEOREM 2.7. *If $t_c + t_a < t_p$, and $p_{ua} + p_{ic} < \alpha$, then it is impossible to implement a read/write data object under a (t_p, α) -partition while achieving (t_c, p_{ic}) -consistency, and (t_a, p_{ua}) -latency, i.e., there exists an execution such that these three properties cannot be satisfied simultaneously.*

PROOF. The proof is by contradiction. In a system that satisfies all three properties in all executions, consider an execution with only two clients, a writer client and a reader client. The execution contains alternating pairs of write and read operations $W_1, R_1, W_2, R_2, \dots, W_n, R_n$, such that:

- Write W_i starts at time $(t_c + t_a) \cdot (i - 1)$,
- Read R_i starts at time $(t_c + t_a) \cdot (i - 1) + t_c$, and
- Each write W_i writes a distinct value v_i .

By our definition of (t_p, α) -partition, there are at least $n \cdot \alpha$ written values v_j 's that have propagation delay $> t_p$. By a similar argument as in the proof of Theorem 2.6, each of their corresponding reads R_j are such that R_j cannot both satisfy t_c -freshness and also return within t_a . That is, R_j is either t_c -stale or returns later than t_a after its start time. There are $n \cdot \alpha$ such reads R_j ; let us call these "bad" reads.

By definition, the set of reads S that are t_c -stale, and the set of reads A that return after t_a are such that $|S| \leq n \cdot p_{ic}$ and $|A| \leq n \cdot p_{ua}$. Put together, these imply:

$$n \cdot \alpha \leq |S \cup A| \leq |S| + |A| \leq n \cdot p_{ic} + n \cdot p_{ua}.$$

The first inequality arises because all the "bad" reads are in $S \cup A$. But this inequality implies that $\alpha \leq p_{ua} + p_{ic}$, which violates our assumptions. \square

3. PCAP KEY-VALUE STORES

Having formally specified the (un)achievable envelope of consistency-latency (Theorem 2.7), we now move our attention to designing systems that achieve performance close to this theoretical envelope. We also convert our probabilistic models for consistency and latency from Section 2

into SLAs, and show how to design adaptive key-value stores that satisfy such probabilistic SLAs inside a single data-center. We call such systems PCAP systems. So PCAP systems (1) can achieve performance close to the theoretical consistency-latency tradeoff envelope, and (2) can adapt to meet probabilistic consistency and latency SLAs inside a single data-center. Our PCAP systems can also alternatively be used with SLAs from PBS [Bailis et al. 2014] or Pileus [Terry et al. 2013; Ardekani and Terry 2014].

Assumptions about underlying Key-value Store. PCAP systems can be built on top of existing key-value stores. We make a few assumptions about such key-value stores. First, we assume that each key is replicated on multiple servers. Second, we assume the existence of a “coordinator” server that acts as a client proxy in the system, finds the replica locations for a key (e.g., using consistent hashing [Stoica et al. 2001]), forwards client queries to replicas, and finally relays replica responses to clients. Most key-value stores feature such a coordinator [Lakshman and Malik 2008; Gross 2009]. Third, we assume the existence of a background mechanism such as read repair [De-Candia et al. 2007] for reconciling divergent replicas. Finally, we assume that the clocks on each server in the system are synchronized using a protocol like NTP so that we can use global timestamps to detect stale data (most key-value stores running within a datacenter already require this assumption, e.g., to decide which updates are fresher). It should be noted that our impossibility results in Section 2 do not depend on the accuracy of the clock synchronization protocol. However the sensitivity of the protocol affects the ability of PCAP systems to adapt to network delays. For example, if the servers are synchronized to within 1 ms using NTP, then the PCAP system cannot react to network delays lower than 1 ms.

SLAs. We consider two scenarios, where the SLA specifies either: i) a probabilistic latency requirement, or ii) a probabilistic consistency requirement. In the former case, our adaptive system optimizes the probabilistic consistency while meeting the SLA requirement, whereas in the latter it optimizes probabilistic latency while meeting the SLA. These SLAs are probabilistic, in the sense that they give statistical guarantees to operations over a long duration.

A latency SLA (i) looks as follows:

Given: Latency $SLA = \langle p_{ua}^{sla}, t_a^{sla}, t_c^{sla} \rangle$;
Ensure that: The fraction p_{ua} of reads, whose finish and start times differ by more than t_a^{sla} , is such that: p_{ua} stays below p_{ua}^{sla} ;
Minimize: The fraction p_{ic} of reads which do not satisfy t_c^{sla} -freshness.

This SLA is similar to latency SLAs used in industry today. As an example, consider a shopping cart application [Terry et al. 2013] where the client requires that at most 10% of the operations take longer than 300 ms, but wishes to minimize staleness. Such an application prefers latency over consistency. In our system, this requirement can be specified as the following PCAP latency SLA:

$\langle p_{ua}^{sla}, t_a^{sla}, t_c^{sla} \rangle = \langle 0.1, 300 \text{ ms}, 0 \text{ ms} \rangle$.

A consistency SLA looks as follows:

Given: Consistency $SLA = \langle p_{ic}^{sla}, t_a^{sla}, t_c^{sla} \rangle$;
Ensure that: The fraction p_{ic} of reads that do not satisfy t_c^{sla} -freshness is such that: p_{ic} stays below p_{ic}^{sla} ;
Minimize: The fraction p_{ua} of reads whose finish and start times differ by more than t_a^{sla} .

Note that as mentioned earlier, consistency is defined based on freshness of the value returned by read operations. As an example, consider a web search application that wants to ensure no more

| Increased Knob | Latency | Consistency |
|-------------------|------------|-------------|
| Read Delay | Degrades | Improves |
| Read Repair Rate | Unaffected | Improves |
| Consistency Level | Degrades | Improves |

Fig. 3. Effect of Various Control Knobs.

than 10% of search results return data that is over 500 ms old, but wishes to minimize the fraction of operations taking longer than 100 ms [Terry et al. 2013]. Such an application prefers consistency over latency. This requirement can be specified as the following PCAP consistency SLA:

$$\langle p_{ic}^{sla}, t_a^{sla}, t_c^{sla} \rangle = \langle 0.10, 100 \text{ ms}, 500 \text{ ms} \rangle.$$

Our PCAP system can leverage three control knobs to meet these SLAs: 1) *read delay*, 2) *read repair rate*, and 3) *consistency level*. The last two of these are present in most key-value stores. The first (read delay) has been discussed in previous literature [Swidler 2009; Bailis et al. 2014; Fan et al. 2015; Golab and Wylie 2014; Zawirski et al. 2015].

3.1. Control Knobs

Figure 3 shows the effect of our three control knobs on latency and consistency. We discuss each of these knobs and explain the entries in the table.

The knobs of Figure 3 are all directly or indirectly applicable to the read path in the key-value store. As an example, the knobs pertaining to the Cassandra query path are shown in Fig. 4, which shows the four major steps involved in answering a read query from a front-end to the key-value store cluster: (1) Client sends a read query for a key to a coordinator server in the key-value store cluster; (2) Coordinator forwards the query to one or more replicas holding the key; (3) Response is sent from replica(s) to coordinator; (4) Coordinator forwards response with highest timestamp to client; (5) Coordinator does *read repair* by updating replicas, which had returned older values, by sending them the freshest timestamp value for the key. Step (5) is usually performed in the background.

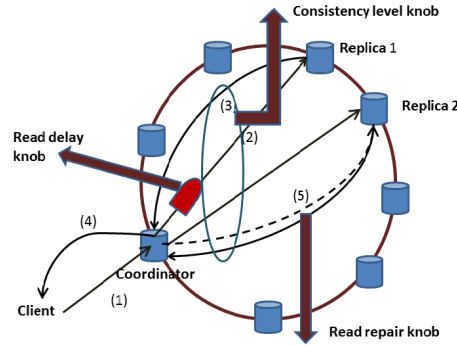


Fig. 4. Cassandra Read Path and PCAP Control Knobs.

A *read delay* involves the coordinator artificially delaying the read query for a specified duration of time before forwarding it to the replicas. i.e., between step (1) and step (2). This gives the system some time to converge after previous writes. Increasing the value of read delay improves consistency (lowers p_{ic}) and degrades latency (increases p_{ua}). Decreasing read delay achieves the reverse. Read delay is an attractive knob because: 1) it does not interfere with client specified parameters (e.g., consistency level in Cassandra [DataStax 2016]), and 2) it can take any non-negative continuous value instead of only discrete values allowed by consistency levels. Our PCAP system inserts read delays only when it is needed to satisfy the specified SLA.

However, read delay cannot be negative, as one cannot speed up a query and send it back in time. This brings us to our second knob: read repair rate. Read repair was depicted as distinct step (5) in our outline of Fig. 4, and is typically performed in the background. The coordinator maintains a buffer of recent reads where some of the replicas returned older values along with the associated freshest value. It periodically picks an element from this buffer and updates the appropriate replicas. In key-value stores like Apache Cassandra and Riak, read repair rate is an accessible configuration parameter per column family.

Our read repair rate knob is the probability with which a given read that returned stale replica values will be added to the read repair buffer. Thus, a read repair rate of 0 implies no read repair, and replicas will be updated only by subsequent writes. Read repair rate = 0.1 means the coordinator performs read repair for 10% of the read requests.

Increasing (respectively, decreasing) the read repair rate can improve (respectively degrade) consistency. Since the read repair rate does not directly affect the read path (Step (5) described earlier, is performed in the background), it does not affect latency. Figure 3 summarizes this behavior.⁴

The third potential control knob is consistency level. Some key-value stores allow the client to specify, along with each read or write operation, how many replicas the coordinator should wait for (in step (3) of Fig. 4) before it sends the reply back in step (4). For instance, Cassandra offers consistency levels: ONE, TWO, QUORUM, ALL. As one increases consistency level from ONE to ALL, reads are delayed longer (latency decreases) while the possibility of returning the latest write rises (consistency increases).

Our PCAP system relies primarily on read delay and repair rate as the control knobs. Consistency level can be used as a control knob only for applications in which user expectations will not be violated, e.g., when reads do not specify a specific discrete consistency level. That is, if a read specifies a higher consistency level, it would be prohibitive for the PCAP system to degrade the consistency level as this may violate client expectations. Techniques like continuous partial quorums (CPQ) [McKenzie et al. 2015], and adaptive hybrid quorums [Davidson et al. 2013] fall in this category, and thus interfere with application/client expectations. Further, read delay and repair rate are *non-blocking* control knobs under replica failure, whereas consistency level is *blocking*. For example, if a Cassandra client sets consistency level to QUORUM with replication factor 3, then the coordinator will be blocked if two of the key's replicas are on failed nodes. On the other hand, under replica failures read repair rate does not affect operation latency, while read delay only delays reads by a maximum amount.

3.2. Selecting A Control Knob

As the primary control knob, the PCAP system prefers read delay over read repair rate. This is because the former allows tuning both consistency and latency, while the latter affects only consistency. The only exception occurs when during the PCAP system adaptation process, a state is reached where consistency needs to be degraded (e.g., increase p_{ic} to be closer to the SLA) but the read delay value is already zero. Since read delay cannot be lowered further, in this instance the PCAP system switches to using the secondary knob of read repair rate, and starts decreasing this instead.

Another reason why read repair rate is not a good choice for the primary knob is that it takes longer to estimate p_{ic} than for read delay. Because read repair rate is a probability, the system needs a larger number of samples (from the operation log) to accurately estimate the actual p_{ic} resulting from a given read repair rate. For example, in our experiments, we observe that the system needs to inject $k \geq 3000$ operations to obtain an accurate estimate of p_{ic} , whereas only $k = 100$ suffices for the read delay knob.

⁴Although read repair rate does not affect latency directly, it introduces some background traffic and can impact propagation delay. While our model ignores such small impacts, our experiments reflect the net effect of the background traffic.

```

1: procedure CONTROL( $\mathcal{S} \mathcal{L} \mathcal{A} = \langle p_{ic}^{sla}, t_c^{sla}, t_a^{sla} \rangle, \epsilon$ )
2:    $p_{ic}^{sla'} := p_{ic}^{sla} - \epsilon$ ;
3:   Select control_knob; // (Sections 3.1, 3.2)
4:    $inc := 1$ ;
5:    $dir = +1$ ;
6:   while (true) do
7:     Inject  $k$  new operations (reads and writes)
8:     into store;
9:     Collect log  $\mathcal{L}$  of recent completed reads
10:    and writes (values, start and finish times);
11:    Use  $\mathcal{L}$  to calculate
12:     $p_{ic}$  and  $p_{ua}$ ; // (Section 3.4)
13:     $new\_dir := (p_{ic} > p_{ic}^{sla'})? +1 : -1$ ;
14:    if  $new\_dir = dir$  then
15:       $inc := inc * 2$ ; // Multiplicative increase
16:      if  $inc > MAX\_INC$  then
17:         $inc := MAX\_INC$ ;
18:      end if
19:    else
20:       $inc := 1$ ; // Reset to unit step
21:       $dir := new\_dir$ ; // Change direction
22:    end if
23:     $control\_knob := control\_knob + inc * dir$ ;
24:  end while
25: end procedure

```

Fig. 5. Adaptive Control Loop for Consistency SLA.

3.3. PCAP Control Loop

The PCAP control loop adaptively tunes control knobs to always meet the SLA under continuously changing network conditions. The control loop for consistency SLA is depicted in Fig. 5. The control loop for a latency SLA is analogous and is not shown.

This control loop runs at a standalone server called the PCAP Coordinator.⁵ This server runs an infinite loop. In each iteration, the coordinator: i) injects k operations into the store (line 6), ii) collects the log \mathcal{L} for the k recent operations in the system (line 8), iii) calculates p_{ua}, p_{ic} (Section 3.4) from \mathcal{L} (line 10), and iv) uses these to change the knob (lines 12-22).

The behavior of the control loop in Fig. 5 is such that the system will converge to “around” the specified SLA. Because our original latency (consistency) SLAs require p_{ua} (p_{ic}) to stay below the SLA, we introduce a *laxity* parameter ϵ , subtract ϵ from the target SLA, and treat this as the target SLA in the control loop. Concretely, given a target consistency SLA $\langle p_{ic}^{sla}, t_a^{sla}, t_c^{sla} \rangle$, where the goal is to control the fraction of stale reads to be under p_{ic}^{sla} , we control the system such that p_{ic} quickly converges around $p_{ic}^{sla'} = p_{ic}^{sla} - \epsilon$, and thus stay below p_{ic}^{sla} . Small values of ϵ suffice to guarantee convergence (for instance, our experiments use $\epsilon \leq 0.05$).

We found that the naive approach of changing the control knob by the smallest unit increment (e.g., always 1 ms changes in read delay) resulted in a long convergence time. Thus, we opted for a *multiplicative* approach (Fig. 5, lines 12-22) to ensure quick convergence.

We explain the control loop via an example. For concreteness, suppose only the read delay knob (Section 3.1) is active in the system, and that the system has a consistency SLA. Suppose p_{ic} is

⁵The PCAP Coordinator is a special server, and is different from Cassandra’s use of a coordinator for clients to send reads and writes.

higher than $p_{ic}^{sl_d}$. The multiplicative-change strategy starts incrementing the read delay, initially starting with a unit step size (line 3). This step size is exponentially *increased* from one iteration to the next, thus multiplicatively increasing read delay (line 14). This continues until the measured p_{ic} goes just under $p_{ic}^{sl_d}$. At this point, the *new_dir* variable changes sign (line 12), so the strategy reverses direction, and the step is reset to unit size (lines 19-20). In subsequent iterations, the read delay starts *decreasing* by the step size. Again, the step size is increased exponentially until p_{ic} just goes above $p_{ic}^{sl_d}$. Then its direction is reversed again, and this process continues similarly thereafter. Notice that (lines 12-14) from one iteration to the next, as long as p_{ic} continues to remain above (or below) $p_{ic}^{sl_d}$, we have that: i) the direction of movement does not change, and ii) exponential increase continues. At steady state, the control loop keeps changing direction with a unit step size (bounded oscillation), and the metric stays converged under the SLA. Although advanced techniques such as *time dampening* can further reduce oscillations, we decided to avoid them to minimize control loop tuning overheads. Later in Section 4, we utilized control theoretic techniques for the control loop in geo-distributed settings to reduce excessive oscillations.

In order to prevent large step sizes, we cap the maximum step size (line 15-17). For our experiments, we do not allow read delay to exceed 10 ms, and the unit step size is set to 1 ms.

We preferred active measurement (whereby the PCAP Coordinator injects queries rather than passive due to two reasons: i) the active approach gives the PCAP Coordinator better control on convergence, thus convergence rate is more uniform over time, and ii) in the passive approach if the client operation rate were to become low, then either the PCAP Coordinator would need to inject more queries, or convergence would slow down. Nevertheless, in Section 5.4.7, we show results using a passive measurement approach. Exploration of hybrid active-passive approaches based on an operation rate threshold could be an interesting direction.

Overall our PCAP controller satisfies SASO (Stability, Accuracy, low Settling time, small Over-shoot) control objectives [Hellerstein et al. 2004].

3.4. Complexity of Computing p_{ua} and p_{ic}

We show that the computation of p_{ua} and p_{ic} (line 10, Fig. 5) is efficient. Suppose there are r reads and w writes in the log, thus log size $k = r + w$. Calculating p_{ua} makes a linear pass over the read operations, and compares the difference of their finish and start times with t_a . This takes $O(r) = O(k)$.

p_{ic} is calculated as follows. We first extract and sort all the writes according to start timestamp, inserting each write into a hash table under key $\langle \text{object value, write key, write timestamp} \rangle$. In a second pass over the read operations, we extract its matching write by using the hash table key (the third entry of the hash key is the same as the read's returned value timestamp). We also extract neighboring writes of this matching write in constant time (due to the sorting), and thus calculate t_c -freshness for each read. The first pass takes time $O(r + w + w \log w)$, while the second pass takes $O(r + w)$. The total time complexity to calculate p_{ic} is thus $O(r + w + w \log w) = O(k \log k)$.

4. PCAP FOR GEO-DISTRIBUTED SETTINGS

In this section we extend our PCAP system from a single data-center to multiple geo-distributed data-centers. We call this system GeoPCAP.

4.1. System Model

Assume there are n data-centers. Each data-center stores multiple replicas for each data-item. When a client application submits a query, the query is first forwarded to the data-center closest to the client. We call this data-center the *local* data-center for the client. If the local data-center stores a replica of the queried data item, that replica might not have the latest value, since write operations at other data-centers could have updated the data item. Thus in our system model, the local data-center contacts one or more of other remote data-centers, to retrieve (possibly) fresher values for the data item.

| Consistency/Latency/WAN | Composition | $\forall j, t_a^j = t?$ | Rule |
|-------------------------|-------------|-------------------------|--|
| Latency | QUICKEST | Y | $p_{ua}^c(t) = \prod_j p_{ua}^j, \forall j, t_a^j = t$ |
| Latency | QUICKEST | N | $p_{ua}^c(\min_j t_a^j) \geq \prod_j p_{ua}^j \geq p_{ua}^c(\max_j t_a^j),$ $\min_j t_a^j \leq t_a^c \leq \max_j t_a^j$ |
| Latency | ALL | Y | $p_{ua}^c(t) = 1 - \prod_j (1 - p_{ua}^j), \forall j, t_a^j = t$ |
| Latency | ALL | N | $p_{ua}^c(\min_j t_a^j) \geq 1 - \prod_j (1 - p_{ua}^j) \geq p_{ua}^c(\max_j t_a^j),$ $\min_j t_a^j \leq t_a^c \leq \max_j t_a^j$ |
| Consistency | QUICKEST | Y | $p_{ic}^c(t) = \prod_j p_{ic}^j, \forall j, t_c^j = t$ |
| Consistency | QUICKEST | N | $p_{ic}^c(\min_j t_c^j) \geq \prod_j p_{ic}^j \geq p_{ic}^c(\max_j t_c^j),$ $\min_j t_c^j \leq t_c^c \leq \max_j t_c^j$ |
| Consistency | ALL | Y | $p_{ic}^c(t) = 1 - \prod_j (1 - p_{ic}^j), \forall j, t_c^j = t$ |
| Consistency | ALL | N | $p_{ic}^c(\min_j t_c^j) \geq 1 - \prod_j (1 - p_{ic}^j) \geq p_{ic}^c(\max_j t_c^j),$ $\min_j t_c^j \leq t_c^c \leq \max_j t_c^j$ |
| Consistency-WAN | N. A. | N. A. | $Pr[X + Y \geq t_c + t_p^G] \geq p_{ic} \cdot \alpha^G$ |
| Latency-WAN | N. A. | N. A. | $Pr[X + Y \geq t_a + t_p^G] \geq p_{ua} \cdot \alpha^G$ |

Fig. 6. GeoPCAP Composition Rules.

4.2. Probabilistic Composition Rules

Each data-center is running our PCAP-enabled key-value store. Each such PCAP instance defines per data-center probabilistic latency and consistency models (Section 2). To obtain the global behavior, we need to compose these probabilistic consistency and latency/availability models across different data-centers. This is done by our composition rules.

The composition rules for merging independent latency/consistency models from data-centers check whether the SLAs are met by the composed system. Since single data-center PCAP systems define probabilistic latency and consistency models, our composition rules are also probabilistic in nature. However in reality, our composition rules do not require all data-centers to run PCAP-enabled key-value stores systems. As long as we can measure consistency and latency at each data-center, we can estimate the probabilistic models of consistency/latency at each data-center and use our composition rules to merge them.

We consider two types of composition rules: (1) QUICKEST (Q), where at-least one data-center (e.g., the local or closest remote data-center) satisfies client specified latency or freshness (consistency) guarantees; and (2) ALL (A), where all the data-centers must satisfy latency or freshness guarantees. These two are, respectively, generalizations of Apache Cassandra multi-data-center deployment [Gilmore 2011] consistency levels (CL): LOCAL_QUORUM and EACH_QUORUM.

Compared to Section 2, which analyzed the fraction of executions that satisfy a predicate (the proportional approach), in this section we use a simpler probabilistic approach. This is because although the proportional approach is more accurate, it is more intractable than the probabilistic model in the geo-distributed case.

Our probabilistic composition rules fall into three categories: (1) composing consistency models; (2) composing latency models; and (3) composing a wide-area-network (WAN) partition model with a data-center (consistency or latency) model. The rules are summarized in Figure 6, and we discuss them next.

4.2.1. Composing latency models. Assume there are n data-centers storing the replica of a key with latency models $(t_a^1, p_{ua}^1), (t_a^2, p_{ua}^2), \dots, (t_a^n, p_{ua}^n)$. Let \mathcal{C}^A denote the composed system. Let (p_{ua}^c, t_a^c) denote the latency model of the composed system \mathcal{C}^A . This indicates that the fraction of reads in \mathcal{C}^A that complete within t_a^c time units is at least $(1 - p_{ua}^c)$. This is the latency SLA expected by clients. Let $p_{ua}^c(t)$ denote the probability of missing deadline by t time units in the composed model. Let X_j denote the random variable measuring read latency in data cen-

ter j . Let $E_j(t)$ denote the event that $X_j > t$. By definition we have that, $Pr[E_j(t_a^j)] = p_{ua}^j$, and $Pr[\bar{E}_j(t_a^j)] = 1 - p_{ua}^j$. Let $f_j(t)$ denote the cumulative distribution function (CDF) for X_j . So by definition, $f_j(t_a^j) = Pr[X_j \leq t_a^j] = 1 - Pr[X_j > t_a^j]$. The following theorem articulates the probabilistic latency composition rules:

THEOREM 4.1. *Let n data-centers store the replica for a key with latency models $(t_a^1, p_{ua}^1), (t_a^2, p_{ua}^2), \dots, (t_a^n, p_{ua}^n)$. Let \mathcal{C}^A denote the composed system with latency model (p_{ua}^c, t_a^c) . Then for composition rule *QUICKEST* we have:*

$$\begin{aligned} p_{ua}^c(\min_j t_a^j) &\geq \prod_j p_{ua}^j \geq p_{ua}^c(\max_j t_a^j), \\ \text{and } \min_j t_a^j &\leq t_a^c \leq \max_j t_a^j, \\ \text{where } j &\in \{1, \dots, n\}. \end{aligned} \quad (1)$$

For composition rule *ALL*,

$$\begin{aligned} p_{ua}^c(\min_j t_a^j) &\geq 1 - \prod_j (1 - p_{ua}^j) \geq p_{ua}^c(\max_j t_a^j), \\ \text{and } \min_j t_a^j &\leq t_a^c \leq \max_j t_a^j, \\ \text{where } j &\in \{1, \dots, n\}. \end{aligned} \quad (2)$$

PROOF. We outline the proof for composition rule *QUICKEST*. In *QUICKEST*, a latency deadline t is violated in the composed model when all data-centers miss the t deadline. This happens with probability $p_{ua}^c(t)$ (by definition). We first prove a simpler Case 1, then the general version in Case 2.

Case 1: Consider the simple case where all t_a^j values are identical, i.e., $\forall j, t_a^j = t_a$: $p_{ua}^c(t_a) = Pr[\cap_i E_i(t_a)] = \cap_i Pr[E_i(t_a)] = \prod_i p_{ua}^i$ (assuming independence across data-centers).

Case 2:

Let,

$$t_a^i = \min_j t_a^j \quad (3)$$

Then,

$$\forall j, t_a^j \geq t_a^i \quad (4)$$

Then, by definition of CDF function,

$$\forall j, f_j(t_a^i) \leq f_j(t_a^j) \quad (5)$$

By definition,

$$\forall j, (Pr[X_j \leq t_a^i] \leq Pr[X_j \leq t_a^j]) \quad (6)$$

$$\forall j, (Pr[X_j > t_a^i] \geq Pr[X_j > t_a^j]) \quad (7)$$

Multiplying all,

$$\prod_j Pr[X_j > t_a^i] \geq \prod_j Pr[X_j > t_a^j] \quad (8)$$

But this means,

$$p_{ua}^c(t_a^i) \geq \Pi_j p_{ua}^j \quad (9)$$

$$p_{ua}^c(\min_j t_a^j) \geq \Pi_j p_{ua}^j \quad (10)$$

Similarly, let

$$t_a^k = \max_j t_a^j \quad (11)$$

Then,

$$\forall j, t_a^k \geq t_a^j \quad (12)$$

$$\forall j, (Pr[X_j > t_a^j] \geq Pr[X_j > t_a^k]) \quad (13)$$

$$\Pi_j Pr[X_j > t_a^j] \geq \Pi_j Pr[X_j > t_a^k] \quad (14)$$

$$\Pi_j p_{ua}^j \geq p_{ua}^c(t_a^k) \quad (15)$$

$$\Pi_j p_{ua}^j \geq p_{ua}^c(\max_j t_a^j) \quad (16)$$

Finally combining Equations 10, and 16, we get Equation 1.

The proof for composition rule ALL follows similarly. In this case, a latency deadline t is satisfied when all data-centers satisfy the deadline. So a deadline miss in the composed model means at-least one data-center misses the deadline. The derivation of the composition rules are similar and we invite the reader to work them out to arrive at the equations depicted in Figure 6. \square

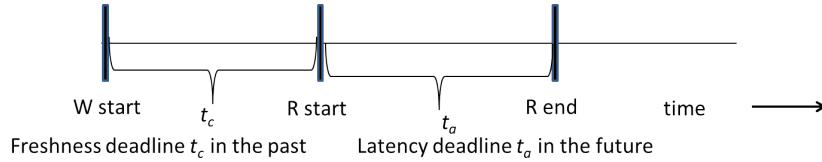


Fig. 7. Symmetry of freshness and latency requirements.

4.2.2. Composing consistency models. t -latency (Definition 2.3) and t -freshness (Definitions 2.1) guarantees are time-symmetric (Figure 7). While t -lateness can be considered a deadline in the future, t -freshness can be considered a deadline in the past. This means that for a given read, t -freshness constrains how old a read value can be. So the composition rules remain the same for consistency and availability.

Thus the consistency composition rules can be obtained by substituting p_{ua} with p_{ic} and t_a with t_c in the latency composition rules (last 4 rows in Table 6).

This leads to the following theorem for consistency composition:

THEOREM 4.2. *Let n data-centers store the replica for a key with consistency models $(t_c^1, p_{ic}^1), (t_c^2, p_{ic}^2), \dots, (t_c^n, p_{ic}^n)$. Let \mathcal{C}^A denote the composed system with consistency model (p_{ic}^c, t_c^c) . Then for composition rule QUICKEST we have:*

$$\begin{aligned}
p_{ic}^c(\min_j t_c^j) &\geq \prod_j p_{ic}^j \geq p_{ic}^c(\max_j t_c^j), \\
\text{and } \min_j t_c^j &\leq t_c^c \leq \max_j t_c^j, \\
\text{where } j &\in \{1, \dots, n\}.
\end{aligned} \tag{17}$$

For composition rule ALL,

$$\begin{aligned}
p_{ic}^c(\min_j t_c^j) &\geq 1 - \prod_j (1 - p_{ic}^j) \geq p_{ic}^c(\max_j t_c^j), \\
\text{and } \min_j t_c^j &\leq t_c^c \leq \max_j t_c^j, \\
\text{where } j &\in \{1, \dots, n\}.
\end{aligned} \tag{18}$$

4.2.3. Composing consistency/latency model with a WAN partition model. All data-centers are connected to each other through a wide-area-network (WAN). We assume the WAN follows a partition model (t_p^G, α^G) . This indicates that α^G fraction of messages passing through the WAN suffers a delay $> t_p^G$. Note that the WAN partition model is distinct from the per data-center partition model (Definition 2.5). Let X denote the latency in a remote data-center, and Y denote the WAN latency of a link connecting the local data-center to this remote data-center (with latency X). Then the total latency of the path to the remote data-center is $X + Y$.⁶

$$Pr[X + Y \geq t_a + t_p^G] \geq (Pr[X \geq t_a] \cdot Pr[Y \geq t_p^G]) = p_{ua} \cdot \alpha^G. \tag{19}$$

Here we assume the WAN latency, and data-center latency distributions are independent. Note that Equation 19 gives a lower bound of the probability. In practice we can estimate the probability by sampling both X and Y , and estimating the number of times $(X + Y)$ exceeds $(t_a + t_p^G)$.

4.3. Example

The example in Figure 8 shows the composition rules in action. In this example, there is one local data-center and 2 replica data-centers. Each data-center can hold multiple replicas of a data-item. First we compose each replica data-center latency model with the WAN partition model. Second we take the WAN-latency composed models for each data-center and compose them using the QUICKEST rule (Figure 6, bottom part).

4.4. GeoPCAP Control Knob

We use a similar delay knob to meet the SLAs in a geo-distributed setting. We call this the *geo-delay* knob and denote it as Δ . The time delay Δ is the delay added at the local data-center to a read request received from a client before it is forwarded to the replica data-centers. Δ affects the consistency-latency trade-off in a manner similar to the read delay knob in a data-center (Section 3.1). Increasing the knob tightens the deadline at each replica data-center, thus increasing per data-center latency (p_{ua}). Similar to read delay (Figure 3), increasing the geo delay knob improves consistency, since it gives each data-center time to commit latest writes.

4.5. GeoPCAP Control Loop

Our GeoPCAP system uses a control loop depicted in Figure 9 for the Consistency SLA case using the QUICKEST composition rule. The control loops for the other three combinations (Consistency-QUICKEST, Latency-ALL, Latency-QUICKEST) are similar.

Initially, we opted to use the single data-center multiplicative control loop (Section 3.3) for GeoPCAP. However, the multiplicative approach led to increased oscillations for the composed consis-

⁶We ignore the latency of the local data-center in this rule, since the local data-center latency is used in the latency composition rule (Section 4.2.1).

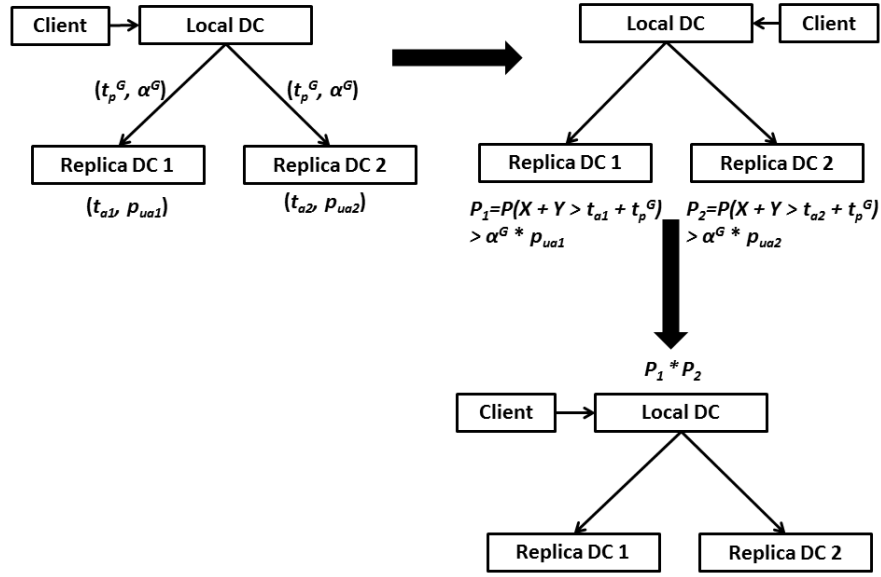


Fig. 8. Example of composition rules in action.

```

1: procedure CONTROL( $\mathcal{S} \mathcal{L} \mathcal{A} = \langle p_{ic}^{sla}, t_c^{sla}, t_a^{sla} \rangle$ )
2:   Geo-delay  $\Delta := 0$ 
3:    $E := 0, Error_{old} := 0$ 
4:   set  $k_p, k_d, k_i$  for PID control (tuning)
5:   Let  $(t_p^G, \alpha^G)$  be the WAN partition model
6:   while (true) do
7:     for each data-center  $i$  do
8:       Let  $F_i$  denote the random freshness interval at  $i$ 
9:       Let  $L_i$  denote the random operation latency at  $i$ 
10:      Let  $W_i$  denote the WAN latency of the link to  $i$ 
11:      Estimate  $p_{ic}^i := Pr[F_i + W_i > t_c^{sla} + t_p^G + \Delta]$  // WAN composition (Section 4.2.3)
12:      Estimate  $p_{ua}^i := Pr[L_i + W_i > t_a + t_p^G - \Delta = t_a^{sla}]$ 
13:    end for
14:     $p_{ic}^c := \prod_i p_{ic}^i, p_{ua}^c := \prod_i p_{ua}^i$  // Consistency/Latency composition (Sections 4.2.1 4.2.2)
15:     $Error := p_{ic}^c - p_{ic}^{sla}$ 
16:     $dE := Error - Error_{old}$ 
17:     $E := E + Error$ 
18:     $u := k_p \cdot Error + k_d \cdot dE + k_i \cdot E$ 
19:     $\Delta := \Delta + u;$ 
20:  end while
21: end procedure

```

Fig. 9. Adaptive Control Loop for GeoPCAP Consistency SLA (QUICKEST Composition).

tency (p_{ic}) and latency (p_{ua}) metrics in a geo-distributed setting. The multiplicative approach sufficed for the single data-center PCAP system, since the oscillations were bounded in a steady-state. However, the increased oscillations in a geo-distributed setting prompted us to use a control theoretic approach for GeoCAP.

As a result, we use a PID control theory approach [Astrom and Hagglund 1995] for the GeoPCAP controller. The controller runs an infinite loop, so that it can react to network delay changes and meet SLAs. There is a tunable sleep time at the end of each iteration (1 sec in Section 5.5 simulations). Initially the geo-delay Δ is set to zero. At each iteration of the loop, we use the composition rules to estimate $p_{ic}^c(t)$, where $t = t_c^{sla} + t_p^G - \Delta$. We also keep track of composed $p_{ua}^c()$ values. We then compute the error, as the difference between current composed p_{ic} and the SLA. Finally the geo-delay change is computed using the PID control law [Astrom and Hagglund 1995] as follows:

$$u = k_p \cdot Error(t) + k_d \cdot \frac{dError(t)}{dt} + k_i \cdot \int Error(t) dt \quad (20)$$

Here, k_p , k_d , k_i represent the proportional, differential, and integral gain factors for the PID controller respectively. There is a vast amount of literature on tuning these gain factors for different control systems [Astrom and Hagglund 1995]. Later in our experiments, we discuss how we set these factors to get SLA convergence. Finally at the end of the iteration, we increase Δ by u . Note that u could be negative, if the metric is less than the SLA.

Note that for the single data-center PCAP system, we used a multiplicative control loop (Section 3.3), which outperformed the unit step size policy. For GeoPCAP, we employ a PID control approach. PID is preferable to the multiplicative approach, since it guarantees fast convergence, and can reduce oscillation to arbitrarily small amounts. However PID's stability depends on proper tuning of the gain factors, which can result in high management overhead. On the other hand the multiplicative control loop has a single tuning factor (the multiplicative factor), so it is easier to manage. Later in Section 5.5 we experimentally compare the PID and multiplicative control approaches.

5. EXPERIMENTS

5.1. Implementation Details

In this section, we discuss how support for our consistency and latency SLAs can be easily incorporated into the Cassandra and Riak key-value stores (in a single data-center) via minimal changes.

5.1.1. PCAP Coordinator. From Section 3.3, recall that the PCAP Coordinator runs an infinite loop that continuously injects operations, collects logs ($k = 100$ operations by default), calculates metrics, and changes the control knob. We implemented a modular PCAP Coordinator using Python (around 100 LOC), which can be connected to any key-value store.

We integrated PCAP into two popular NoSQL stores: Apache Cassandra [Lakshman and Malik 2008] and Riak [Gross 2009] – each of these required changes to about 50 lines of original store code.

5.1.2. Apache Cassandra. First, we modified the Cassandra v1.2.4 to add read delay and read repair rate as control knobs. We changed the Cassandra Thrift interface so that it accepts read delay as an additional parameter. Incorporating the read delay into the read path required around 50 lines of Java code.

Read repair rate is specified as a column family configuration parameter, and thus did not require any code changes. We used YCSB's Cassandra connector as the client, modified appropriately to talk with the clients and the PCAP Coordinator.

5.1.3. Riak. We modified Riak v1.4.2 to add read delay and read repair as control knobs. Due to the unavailability of a YCSB Riak connector, we wrote a separate YCSB client for Riak from scratch (250 lines of Java code). We decided to use YCSB instead of existing Riak clients, since YCSB offers flexible workload choices that model real world key-value store workloads.

We introduced a new system-wide parameter for read delay, which was passed via the Riak http interface to the Riak coordinator which in turn applied it to all queries that it receives from clients. This required about 50 lines of Erlang code in Riak. Like Cassandra, Riak also has built-in support for controlling read repair rate.

5.2. Experiment Setup

Our experiments are in three stages: microbenchmarks for a single data-center (Section 5.3) and deployment experiments for a single data-center (Section 5.4), and a realistic simulation for the geo-distributed setting (Section 5.5). We first discuss the experiments for a single data-center setting.

Our single data-center PCAP Cassandra system and our PCAP Riak system were each run with their default settings. We used YCSB v 0.1.4 [Cooper et al. 2010b] to send operations to the store. YCSB generates synthetic workloads for key-value stores and models real-world workload scenarios (e.g., Facebook photo storage workload). It has been used to benchmark many open-source and commercial key-value stores, and is the de facto benchmark for key-value stores [Cooper et al. 2010a].

Each YCSB experiment consisted of a load phase, followed by a work phase. Unless otherwise specified, we used the following YCSB parameters: 16 threads per YCSB instance, 2048 B values, and a read-heavy distribution (80% reads). We had as many YCSB instances as the cluster size, one co-located at each server. The default key size was 10 B for Cassandra, and Riak. Both YCSB-Cassandra and YCSB-Riak connectors were used with the weakest quorum settings and 3 replicas per key. The default throughput was 1000 ops/s. All operations use a consistency level of ONE.

Both PCAP systems were run in a cluster of 9 d710 Emulab servers [White et al. 2002], each with 4 core Xeon processors, 12 GB RAM, and 500 GB disks. The default network topology was a LAN (star topology), with 100 Mbps bandwidth and inter-server round-trip delay of 20 ms, dynamically controlled using traffic shaping.

We used NTP to synchronize clocks within 1 ms. This is reasonable since we are limited to a single data-center. This clock skew can be made tighter by using atomic or GPS clocks [Corbett et al. 2012]. This synchronization is needed by the PCAP coordinator to compute the SLA metrics.

5.3. Microbenchmark Experiments (Single Data-center)

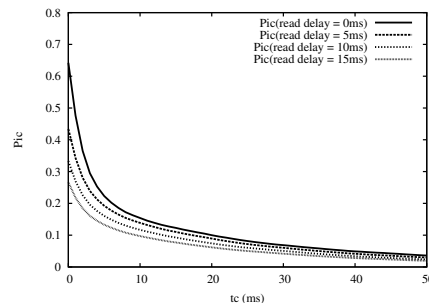


Fig. 10. Effectiveness of Read Delay knob in PCAP Cassandra. Read repair rate fixed at 0.1.

5.3.1. Impact of Control Knobs on Consistency. We study the impact of two control knobs on consistency: read delay and read repair rate.

Fig. 10 shows the inconsistency metric p_{ic} against t_c for different read delays. This shows that when applications desire fresher data (left half of the plot), read delay is flexible knob to control inconsistency p_{ic} . When the freshness requirements are lax (right half of plot), the knob is less useful. However, p_{ic} is already low in this region.

On the other hand, read repair rate has a relatively smaller effect. We found that a change in read repair rate from 0.1 to 1 altered p_{ic} by only 15%, whereas Fig. 10 showed that a 15 ms increase in read delay (at $t_c = 0$ ms) lowered inconsistency by over 50%. As mentioned earlier, using read repair

rate requires calculating p_{ic} over logs of at least $k = 3000$ operations, whereas read delay worked well with $k = 100$. Henceforth, by default we use read delay as our sole control knob.

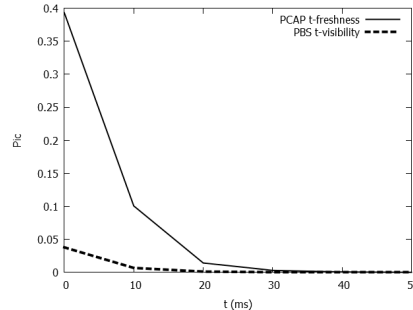


Fig. 11. p_{ic} PCAP vs. PBS consistency metrics. Read repair rate set to 0.1, 50% writes.

5.3.2. PCAP vs. PBS. To show that our system can work with PBS [Bailis et al. 2014], we integrated t -visibility into PCAP. Fig. 11 compares, for a 50%-write workload, the probability of inconsistency against t for both existing work PBS (t -visibility) [Bailis et al. 2014] and PCAP (t -freshness) described in Section 2.1. We observe that PBS’s reported inconsistency is lower compared to PCAP. This is because, PBS considers a read that returns the value of an in-flight write (overlapping read and write) to be always fresh, by default. However the comparison between PBS and PCAP metrics is not completely fair, since the PBS metric is defined in terms of write operation end times, whereas our PCAP metric is based on write start times. It should be noted that the purpose of this experiment is not to show which metric captures client-centric consistency better. Rather, our goal is to demonstrate that our PCAP system can be made to run by using PBS t -visibility metric instead of PCAP t -freshness.

5.3.3. PCAP Metric Computation Time. Fig. 12 shows the total time for the PCAP Coordinator to calculate p_{ic} and p_{ua} metrics for values of k from 100 to 10K, and using multiple threads. We observe low computation times of around 1.5 s, except when there are 64 threads and a 10K-sized log: under this situation, the system starts to degrade as too many threads contend for relatively few memory resources. Henceforth, the PCAP Coordinator by default uses a log size of $k = 100$ operations and 16 threads.

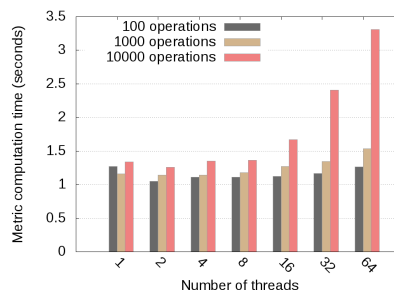


Fig. 12. PCAP Coordinator time taken to both collect logs and compute p_{ic} and p_{ua} in PCAP Cassandra.

| System | SLA | Parameters | Delay Model | Plot |
|-----------|-------------|---|------------------|----------------------|
| Riak | Latency | $p_{ua} = 0.2375, t_a = 150 \text{ ms}, t_c = 0 \text{ ms}$ | Sharp delay jump | Fig. 17 |
| Riak | Consistency | $p_{ic} = 0.17, t_c = 0 \text{ ms}, t_a = 150 \text{ ms}$ | Lognormal | Fig. 21 |
| Cassandra | Latency | $p_{ua} = 0.2375, t_a = 150 \text{ ms}, t_c = 0 \text{ ms}$ | Sharp delay jump | Figs. 14, 15, 16 |
| Cassandra | Consistency | $p_{ic} = 0.15, t_c = 0 \text{ ms}, t_a = 150 \text{ ms}$ | Sharp delay jump | Fig. 18 |
| Cassandra | Consistency | $p_{ic} = 0.135, t_c = 0 \text{ ms}, t_a = 200 \text{ ms}$ | Lognormal | Figs. 19, 20, 25, 26 |
| Cassandra | Consistency | $p_{ic} = 0.2, t_c = 0 \text{ ms}, t_a = 200 \text{ ms}$ | Lognormal | Fig. 27 |
| Cassandra | Consistency | $p_{ic} = 0.125, t_c = 0 \text{ ms}, t_a = 25 \text{ ms}$ | Lognormal | Figs. 22, 23 |
| Cassandra | Consistency | $p_{ic} = 0.12, t_c = 3 \text{ ms}, t_a = 200 \text{ ms}$ | Lognormal | Figs. 28, 29 |
| Cassandra | Consistency | $p_{ic} = 0.12, t_c = 3 \text{ ms}, t_a = 200 \text{ ms}$ | Lognormal | Figs. 30, 31 |

Fig. 13. *Deployment Experiments: Summary of Settings and Parameters.*

5.4. Deployment Experiments

We now subject our two PCAP systems to network delay variations and YCSB query workloads. In particular, we present two types of experiments: 1) *sharp network jump* experiments, where the network delay at some of the servers changes suddenly, and 2) *lognormal* experiments, which inject continuously-changing and realistic delays into the network. Our experiments use $\epsilon \leq 0.05$ (Section 3.3).

Fig. 13 summarizes the various of SLA parameters and network conditions used in our experiments.

5.4.1. Latency SLA under Sharp Network Jump. Fig. 14 shows the timeline of a scenario for PCAP Cassandra using the following latency SLA: $p_{ua}^{sla} = 0.2375, t_c = 0 \text{ ms}, t_a = 150 \text{ ms}$.

In the initial segment of this run ($t = 0 \text{ s}$ to $t = 800 \text{ s}$) the network delays are small; the one-way server-to-LAN switch delay is 10 ms (this is half the machine to machine delay, where a machine can be either a client or a server). After the warm up phase, by $t = 400 \text{ s}$, Fig. 14 shows that p_{ua} has converged to the target SLA. Inconsistency p_{ic} stays close to zero.

We wish to measure how close the PCAP system is to the optimal-achievable envelope (Section 2). The envelope captures the lowest possible values for consistency (p_{ic}, t_c), and latency (p_{ua}, t_a), allowed by the network partition model (α, t_p) (Theorem 2.7). We do this by first calculating α for our specific network, then calculating the optimal achievable non-SLA metric, and finally seeing how close our non-SLA metric is to this optimal.

First, from Theorem 2.6 we know that the achievability region requires $t_c + t_a \geq t_p$; hence, we set $t_p = t_c + t_a$. Based on this, and the probability distribution of delays in the network, we calculate analytically the exact value of α as the fraction of client pairs whose propagation delay exceeds t_p (see Definition 2.5).

Given this value of α at time t , we can calculate the optimal value of p_{ic} as $p_{ic}(opt) = \max(0, \alpha - p_{ua})$. Fig. 14 shows that in the initial part of the plot (until $t = 800 \text{ s}$), the value of α is close to 0, and the p_{ic} achieved by PCAP Cassandra is close to optimal.

At time $t = 800 \text{ s}$ in Fig. 14, we sharply increase the one-way server-to-LAN delay for 5 out of 9 servers from 10 ms to 26 ms. This sharp network jump results in a lossier network, as shown by the value of α going up from 0 to 0.42. As a result, the value of p_{ua} initially spikes – however, the PCAP system adapts, and by time $t = 1200 \text{ s}$ the value of p_{ua} has converged back to under the SLA.

However, the high value of $\alpha (= 0.42)$ implies that the optimal-achievable $p_{ic}(opt)$ is also higher after $t = 800 \text{ s}$. Once again we notice that p_{ic} converges in the second segment of Fig. 14 by $t = 1200 \text{ s}$.

To visualize how close the PCAP system is to the optimal-achievable envelope, Fig. 15 shows the two achievable envelopes as piecewise linear segments (named “before jump” and “after jump”) and the (p_{ua}, p_{ic}) data points from our run in Fig. 14. The figure annotates the clusters of data points by their time interval. We observe that in the stable states both before the jump (dark circles) and after the jump (empty triangles) are close to their optimal-achievable envelopes.

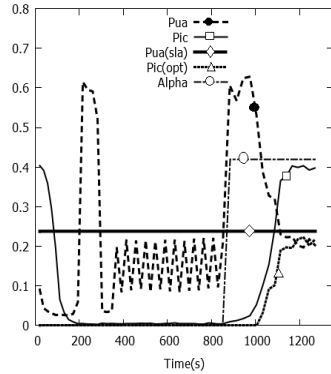


Fig. 14. Latency SLA with PCAP Cassandra under Sharp Network Jump at 800 s: Timeline.

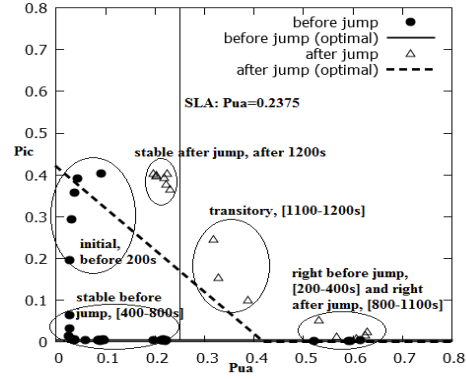


Fig. 15. Latency SLA with PCAP Cassandra under Sharp Network Jump: Consistency-Latency Scatter plot.

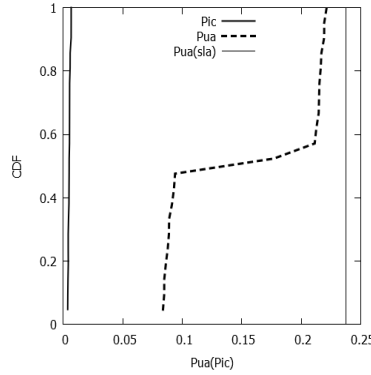


Fig. 16. Latency SLA with PCAP Cassandra under Sharp Network Jump: Steady State CDF [400 s, 800 s].

Fig. 16 shows the CDF plot for p_{ua} and p_{ic} in the steady state time interval [400 s, 800 s] of Fig. 14, corresponding to the bottom left cluster from Fig. 15. We observe that p_{ua} is always below the SLA.

Fig. 17 shows a scatter plot for our PCAP Riak system under a latency SLA ($p_{ua}^{sla} = 0.2375$, $t_a = 150$ ms, $t_c = 0$ ms). The sharp network jump occurs at time $t = 4300$ s when we increase the one-way server-to-LAN delay for 4 out of the 9 Riak nodes from 10 ms to 26 ms. It takes about 1200 s for p_{ua} to converge to the SLA (at around $t = 1400$ s in the warm up segment and $t = 5500$ s in the second segment).

5.4.2. Consistency SLA under Sharp Network Jump. We present consistency SLA results for PCAP Cassandra (PCAP Riak results are similar and are omitted). We use $p_{ic}^{sla} = 0.15$, $t_c = 0$ ms, $t_a = 150$ ms. The initial one-way server-to-LAN delay is 10 ms. At time 750 s, we increase the one-way server-to-LAN delay for 5 out of 9 nodes to 14 ms. This changes α from 0 to 0.42.

Fig. 18 shows the scatter plot. First, observe that the PCAP system meets the consistency SLA requirements, both before and after the jump. Second, as network conditions worsen, the optimal-achievable envelope moves significantly. Yet the PCAP system remains close to the optimal-achievable envelope. The convergence time is about 100 s, both before and after the jump.

5.4.3. Experiments with Realistic Delay Distributions. This section evaluates the behavior of PCAP Cassandra and PCAP Riak under continuously-changing network conditions and a consistency SLA (latency SLA experiments yielded similar results and are omitted).

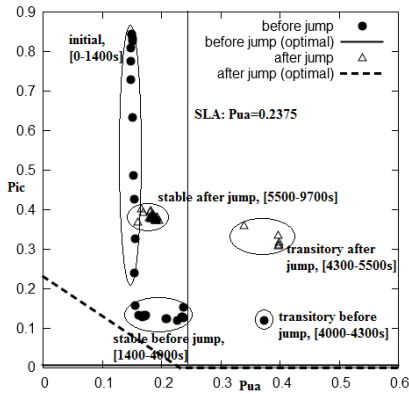


Fig. 17. Latency SLA with PCAP Riak under Sharp Network Jump: Consistency-Latency Scatter plot.

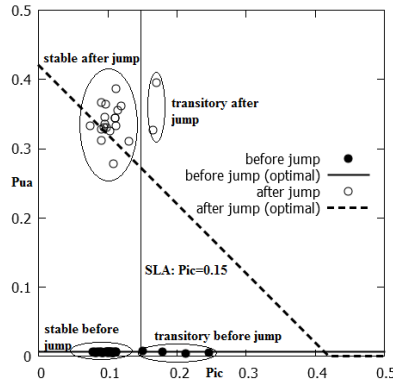


Fig. 18. Consistency SLA with PCAP Cassandra under Sharp Network Jump: Consistency-Latency Scatter plot.

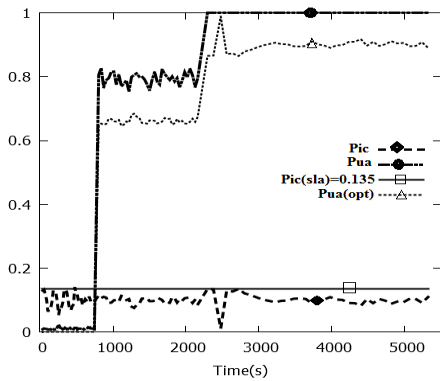


Fig. 19. Consistency SLA with PCAP Cassandra under Lognormal delay distribution: Timeline.

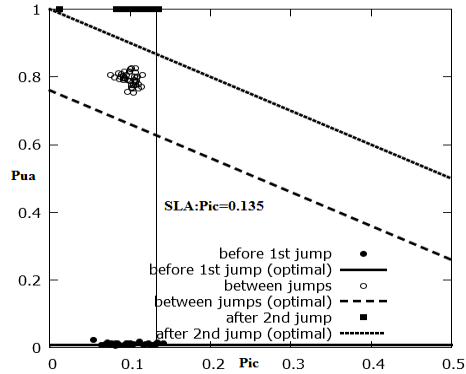


Fig. 20. Consistency SLA with PCAP Cassandra under Lognormal delay distribution: Consistency-Latency Scatter plot.

Based on studies for enterprise data-centers [Benson et al. 2010] we use a lognormal distribution for injecting packet delays into the network. We modified the Linux traffic shaper to add lognormally distributed delays to each packet. Fig. 19 shows a timeline where initially ($t = 0$ to 800 s) the delays

are lognormally distributed, with the underlying normal distributions of $\mu = 3$ ms and $\sigma = 0.3$ ms. At $t = 800$ s we increase μ and σ to 4 ms and 0.4 ms respectively. Finally at around 2100 s, μ and σ become 5 ms and 0.5 ms respectively. Fig. 20 shows the corresponding scatter plot. We observe that in all three time segments, the inconsistency metric p_{ic} : i) stays below the SLA, and ii) upon a sudden network change converges back to the SLA. Additionally, we observe that p_{ua} converges close to its optimal achievable value.

Fig. 21 shows the effect of worsening network conditions on PCAP Riak. At around $t = 1300$ s we increase μ from 1 ms to 4 ms, and σ from 0.1 ms to 0.5 ms. The plot shows that it takes PCAP Riak an additional 1300 s to have inconsistency p_{ic} converge to the SLA. Further the non-SLA metric p_{ua} converges close to the optimal.

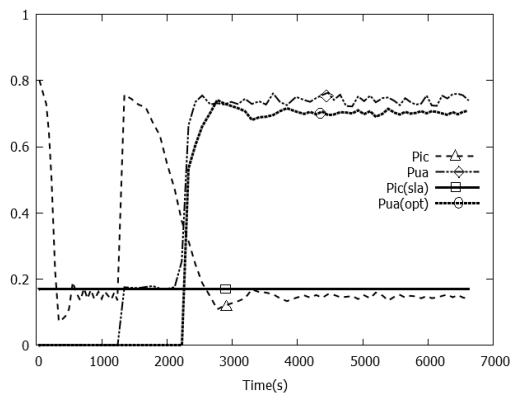


Fig. 21. Consistency SLA with PCAP Riak under Lognormal delay distribution: Timeline.

So far all of our experiments used lax timeliness requirements ($t_a = 150$ ms, 200 ms), and were run on top of relatively high delay networks. Next we perform a stringent consistency SLA experiment ($t_c = 0$ ms, $p_{ic} = .125$) with a very tight latency timeliness requirement ($t_a = 25$ ms). Packet delays are still lognormally distributed, but with lower values. Fig. 22 shows a timeline where initially the delays are lognormally distributed with $\mu = 1$ ms, $\sigma = 0.1$ ms. At time $t = 160$ s we increase μ and σ to 1.5 ms and 0.15 ms respectively. Then at time $t = 320$ s, we decrease μ and σ to return to the initial network conditions. We observe that in all three time segments, p_{ic} stays below the SLA, and quickly converges back to the SLA after a network change. Since the network delays are very low throughout the experiment, α is always 0. Thus the optimal p_{ua} is also 0. We observe that p_{ua} converges very close to optimal before the first jump and after the second jump ($\mu = 1$ ms, $\sigma = 0.1$ ms). In the middle time segment ($t = 160$ to 320 s), p_{ua} degrades in order to meet the consistency SLA under slightly higher packet delays. Fig. 23 shows the corresponding scatter plot. We observe that the system is close to the optimal envelope in the first and last time segments, and the SLA is always met. We note that we are far from optimal in the middle time segment, when the network delays are slightly higher. This shows that when the network conditions are relatively good, the PCAP system is close to the optimal envelope, but when situations worsen we move away. The gap between the system performance and the envelope indicates that the bound (Theorem 2.7) could be improved further. We leave this as an open question.

5.4.4. Effect of Read Repair Rate Knob. All of our deployment experiments use read delay as the only control knob. Fig. 24 shows a portion of a run when only read repair rate was used by our PCAP Cassandra system. This was because read delay was already zero, and we needed to push p_{ic} up to p_{ic}^{sla} . First we notice that p_{ua} does not change with read repair rate, as expected (Figure. 3). Second, we notice that the convergence of p_{ic} is very slow – it changes from 0.25 to 0.3 over a long period of 1000 s.

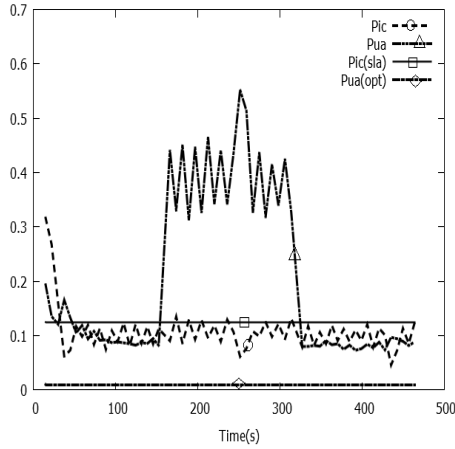


Fig. 22. Consistency SLA
 $(t_c = 0 \text{ ms}, p_{ic} = 0.125, t_a = 25 \text{ ms})$
 with PCAP Cassandra under Lognormal
 delay (low) distribution: Timeline.

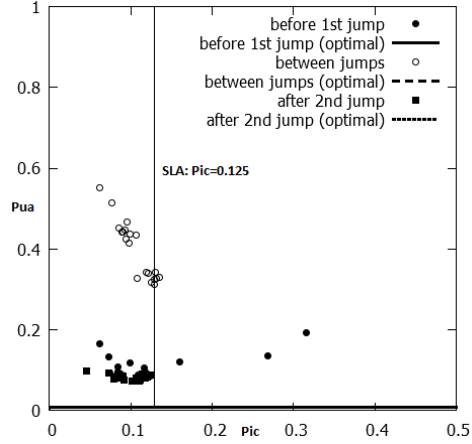


Fig. 23. Consistency SLA
 $(t_c = 0 \text{ ms}, p_{ic} = 0.125, t_a = 25 \text{ ms})$
 with PCAP Cassandra under Lognormal
 delay (low) distribution: Scatter Plot.

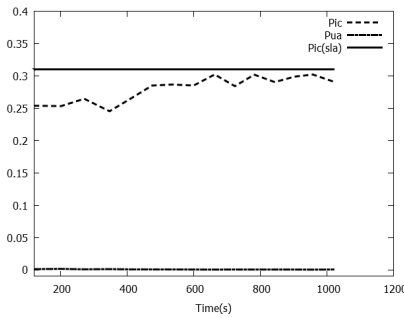


Fig. 24. Effect of Read Repair Rate on PCAP Cassandra. $p_{ic} = 0.31, t_c = 0 \text{ ms}, t_a = 100 \text{ ms}$.

Due to this slow convergence, we conclude that read repair rate is useful only when network delays remain relatively stable. Under continuously changing network conditions (e.g., a lognormal distribution) convergence may be slower and thus read delay should be used as the only control knob.

5.4.5. Scalability. We measure scalability via an increased workload on PCAP Cassandra. Compared to Fig. 20, in this new run we increased the number of servers from 9 to 32, and throughput to 16000 ops/s, and ensured that each server stores at least some keys. All other settings are unchanged compared to Fig. 20. The result is shown Fig. 25. Compared with Fig. 20, we observe an improvement with scale – in particular, increasing the number of servers brings the system closer to optimal. As the number of servers in the system increase, the chance of finding a replica server close to a client proxy also increases. This in turn lowers read latency, thus bringing the system closer to the optimal envelope.

5.4.6. Effect of Timeliness Requirement. The timeliness requirements in an SLA directly affect how close the PCAP system is to the optimal-achievable envelope. Fig. 26 shows the effect of varying the timeliness parameter t_a in a consistency SLA ($t_c = 0 \text{ ms}, p_{ic} = 0.135$) experiment for PCAP Cassandra with 10 ms node to LAN delays. For each t_a , we consider the cluster of the (p_{ua}, p_{ic}) points achieved by the PCAP system in its stable state, calculate its centroid, and measure (and

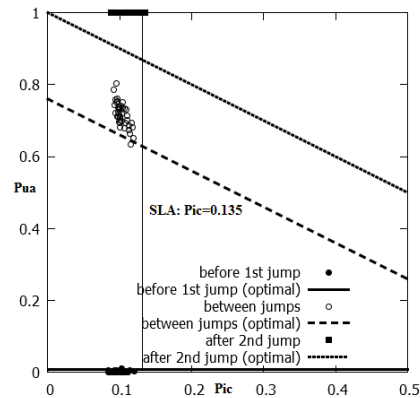


Fig. 25. Scatter plot for same settings as Fig. 20, but with 32 servers and 16K ops/s.

plot on vertical axis) the distance d from this centroid to the optimal-achievable consistency-latency envelope. Note that the optimal envelope calculation also involves t_a , since α depends on it (Section 5.4.1).

Fig. 26 shows that when t_a is too stringent (< 100 ms), the PCAP system may be far from the optimal envelope even when it satisfies the SLA. In the case of Fig. 26, this is because in our network, the average time to cross four hops (client to coordinator to replica, and the reverse) is $20 \times 4 = 80$ ms.⁷ As t_a starts to go beyond this (e.g., $t_a \geq 100$ ms), the timeliness requirements are less stringent, and PCAP is essentially optimal (very close to the achievable envelope).

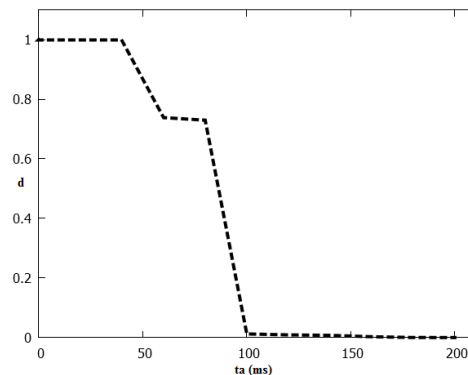


Fig. 26. Effect of Timeliness Requirement (t_a) on PCAP Cassandra. Consistency SLA with $p_{ic} = 0.135$, $t_c = 0$ ms.

5.4.7. Passive Measurement Approach. So far all our experiments have used the active measurement approach. In this section, we repeat a PCAP Cassandra consistency SLA experiment ($p_{ic} = 0.2$, $t_c = 0$ ms) using a passive measurement approach.

In Figure 27, instead of actively injecting operations, we sample ongoing client operations. We estimate p_{ic} and p_{ua} from the 100 latest operations from 5 servers selected randomly.

At the beginning, the delay is lognormally distributed with $\mu = 1$ ms, $\sigma = 0.1$ ms. The passive approach initially converges to the SLA. We change the delay ($\mu = 2$ ms, $\sigma = 0.2$ ms) at $t = 325$ s. We observe that, compared to the active approach, 1) consistency (SLA metric) oscillates more, and

⁷Round-trip time for each hop is $2 \times 10 = 20$ ms.

2) the availability (non-SLA metric) is farther from optimal and takes longer to converge. For the passive approach, SLA convergence and non-SLA optimization depends heavily on the sampling of operations used to estimate the metrics. Thus we conclude that it is harder to satisfy SLA and optimize the non-SLA metric with the passive approach.

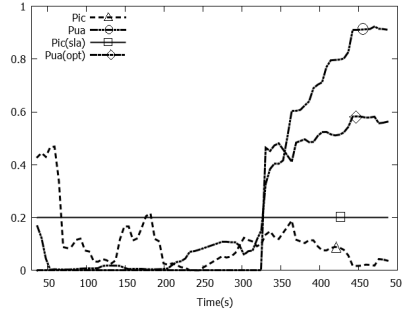


Fig. 27. Consistency SLA with PCAP Cassandra under Lognormal delay distribution: Timeline (Passive).

5.4.8. YCSB Benchmark Experiments. So far we have used YCSB client workloads for all our experiments. Specifically, we used a read-heavy (80% reads) workload. However a 80% read-heavy workload is not one of the standard YCSB benchmark workloads [Cooper et al. 2010c]. Thus to facilitate benchmark comparisons of PCAP with other systems with similar capabilities in the future, we show experimental results for PCAP using two standard YCSB benchmark workloads: (1) Workload A (Update heavy) which has 50/50 reads and writes, and (2) Workload D (Read latest with 95% reads) where most recently inserted records are the most popular.

Read Latest Workload. In this section, we show the results of a PCAP Cassandra consistency SLA experiment ($p_{ic} = 0.12$, $t_c = 3$ ms, $t_a = 200$ ms) using a read latest workload (YCSB workload d). The timeline plot is shown in Figure 28. Initially ($t = 0$ to 380 s) the network delays are lognormally distributed, with the underlying normal distributions of $\mu = 3$ ms and $\sigma = 0.3$ ms. At $t = 380$ s we increase μ and σ to 4 ms and 0.4 ms respectively. Finally at around 1100 s, μ and σ become 5 ms and 0.5 ms respectively. The timeline plots shows that for read-latest workload (with 95% reads), PCAP Cassandra meets the SLA, and also latency p_{ua} converges close to the optimal. This is also evident from the corresponding scatter plot in Figure 29. The trends for read-latest do not exhibit marked differences from our previous experiments with read-heavy workloads (80% reads).

Update Heavy Workload. Next we present results of a PCAP Cassandra consistency SLA experiment ($p_{ic} = 0.12$, $t_c = 3$ ms, $t_a = 200$ ms) using an update heavy workload (YCSB workload a, 50% writes). For this experiment, we increase the average network delay from 3 ms to 4 ms at time 540 s, and from 4 ms to 5 ms at time 1630 s. The timeline plot in Figure 30 indicates poor convergence behavior compared to read-heavy and read-latest distributions. Especially after the second jump, it takes about 1000 s to converge back to SLA. This is because our target key-value stores (Cassandra, Riak) rely heavily on read-repair mechanisms to synchronize replicas in the background. With an update-heavy workload, read-repair synchronization mechanisms lose their effectiveness, which makes it harder to guarantee consistency SLA convergence. The scatter plot in Figure 31 however shows that PCAP Cassandra performs close to the optimal envelope, except for some outliers which are transient states before convergence. It should be noted that an update-heavy workload is not a realistic workload for many key-value stores, and we have only presented results with such workloads for future comparison with other systems using standard benchmarks like YCSB.

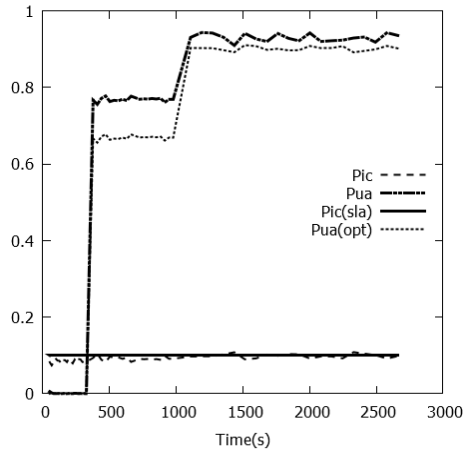


Fig. 28. Consistency SLA
 $(t_c = 3 \text{ ms}, p_{ic} = 0.12, t_a = 200 \text{ ms})$
 with PCAP Cassandra under Lognormal
 delay (latest) distribution: Timeline.

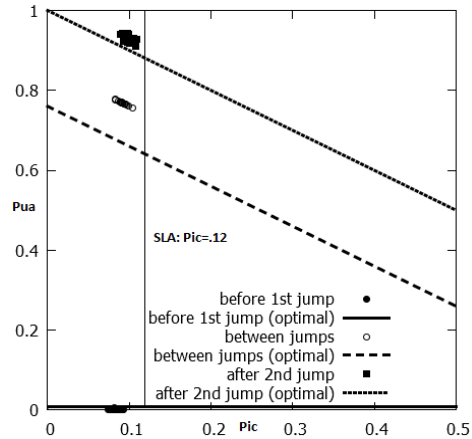


Fig. 29. Consistency SLA
 $(t_c = 3 \text{ ms}, p_{ic} = 0.12, t_a = 200 \text{ ms})$
 with PCAP Cassandra under Lognormal
 delay (latest) distribution: Scatter Plot.

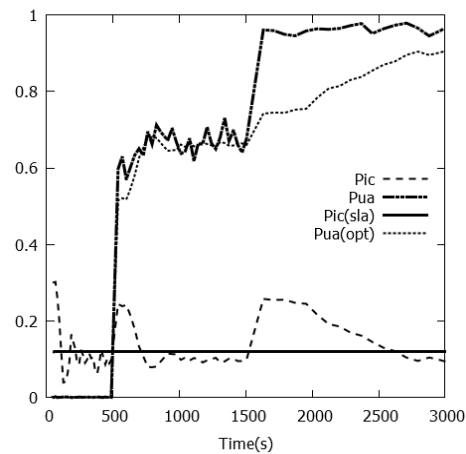


Fig. 30. Consistency SLA
 $(t_c = 3 \text{ ms}, p_{ic} = 0.12, t_a = 200 \text{ ms})$
 with PCAP Cassandra under Lognormal
 delay (update-heavy) distribution: Timeline.

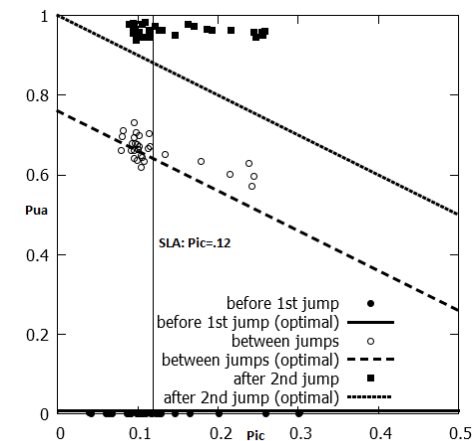


Fig. 31. Consistency SLA
 $(t_c = 3 \text{ ms}, p_{ic} = 0.12, t_a = 200 \text{ ms})$
 with PCAP Cassandra under Lognormal
 delay (update-heavy) distribution: Scatter Plot.

5.5. GeoPCAP Evaluation

We evaluate GeoPCAP with a Monte-Carlo simulation. In our setup, we have four data-centers, among which three are remote data-centers holding replicas of a key, and the fourth one is the local data-center. At each iteration, we estimate t -freshness per data-center using a variation of the well-known WARS model [Bailis et al. 2014]. The WARS model is based on Dynamo style quorum systems [DeCandia et al. 2007], where data staleness is due to read and write message reordering. The model has four components. W represents the message delay from coordinator to replica. The acknowledgment from the replica back to the coordinator is modeled by a random variable A . The read message delay from coordinator to replica, and the acknowledgment back are represented by R , and S , respectively. A read will be stale if a read is acknowledged before a write reaches the replica,

i. e. , $R + S < W + A$. In our simulation, we ignore the A component since we do not need to wait for a write to finish before a read starts. We use the LinkedIn SSD disk latency distribution [Bailis et al. 2014], Table 3 for read/write operation latency values.

We model the WAN delay using a normal distribution $N(20\text{ ms}, \sqrt{2}\text{ ms})$ based on results from Baldoni et al. [2006]. Each simulation runs for 300 iterations. At each iteration, we run the PID control loop (Figure 9) to estimate a new value for geo-delay Δ , and sleep for 1 sec. All reads in the following iteration are delayed at the local data-center by Δ . At iteration 150, we inject a jump by increasing the mean and standard deviation of each WAN link delay normal distribution to 22 ms and $\sqrt{2.2}\text{ ms}$, respectively. We show only results for consistency and latency SLA for the ALL composition. The QUICKEST composition results are similar and are omitted.

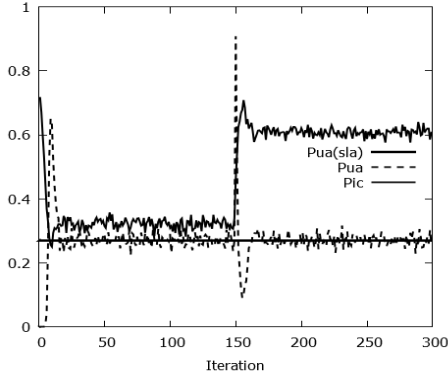


Fig. 32. GeoPCAP SLA Timeline for L SLA (ALL).

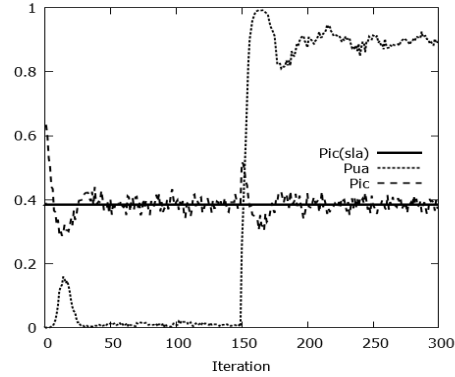


Fig. 33. GeoPCAP SLA Timeline for C SLA (ALL).

Figure 32 shows the timeline of SLA convergence for GeoPCAP Latency SLA ($p_{ua}^{sla} = 0.27, ta^{sla} = 25\text{ ms}, tc^{sla} = 0.1\text{ ms}$). It should be noted that a latency SLA ($p_{ua}^{sla} = 0.27, ta^{sla} = 25\text{ ms}, tc^{sla} = 0.1\text{ ms}$) for GeoPCAP means that when using the ALL composition rule (all individual data-center deployments must satisfy a latency deadline), each single data-center PCAP needs to provide an SLA specified as ($p_{ua}^{sla} = 0.1, ta^{sla} = 25\text{ ms}, tc^{sla} = 0.1\text{ ms}$) (using the composition rule in the third row of Figure 6). We observe that using the PID controller ($k_p = 1, k_d = 0.5, k_i = 0.5$), both the SLA and the other metric converge within 5 iterations initially and also after the jump. Figure 34 shows the corresponding evolution of the geo-delay control knob. Before the jump, the read delay converges to around 5 ms. After the jump, the WAN delay increase forces the geo-delay to converge to a lower value (around 3 ms) in order to meet the latency SLA.

Figure 33 shows the consistency SLA ($p_{ic}^{sla} = 0.38, tc^{sla} = 1\text{ ms}, ta^{sla} = 25\text{ ms}$) time line. Here convergence takes 25 iterations, thanks to the PID controller ($k_p = 1, k_d = 0.8, k_i = 0.5$). We needed a slightly higher value for the differential gain k_d to deal with increased oscillation for the consistency SLA experiment. Note that the p_{ic}^{sla} value of 0.38 forces a smaller per data-center p_{ic} convergence. The corresponding geo-delay evolution (Figure 35) initially converges to around 3 ms before the jump, and converges to around 5 ms after the jump, to enforce the consistency SLA after the delay increase.

We also repeated the Latency SLA experiment with the ALL composition (Figures 32, 34) using the multiplicative control approach (Section 3.3) instead of the PID control approach. Figure 36 shows the corresponding geo-delay trend compared to Figure 34. Comparing the two figures, we observe that although the multiplicative strategy converges as fast the PID approach both before and after the delay jump, the read delay value keeps oscillating around the optimal value. Such oscillations cannot be avoided in the multiplicative approach, since at steady state the control loop

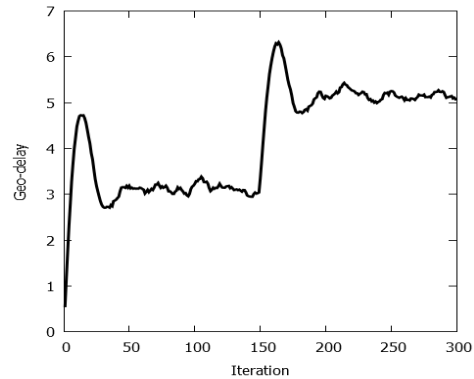
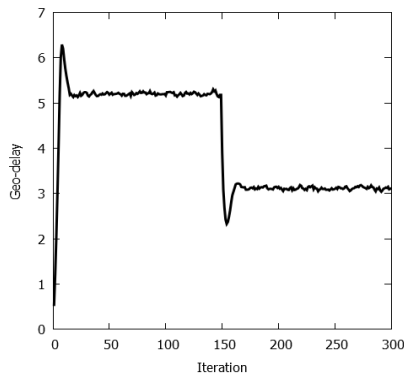


Fig. 34. *Geo-delay Timeline for L SLA (ALL)(Figure 32).* Fig. 35. *Geo-delay Timeline for C SLA (ALL)(Figure 33).*

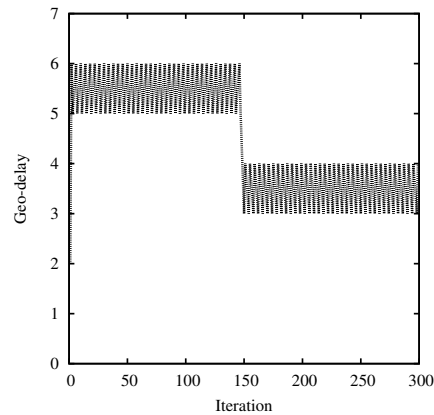


Fig. 36. *Geo-delay Timeline for A SLA (ALL) with Multiplicative Approach.*

keeps changing direction with a unit step size. Compared to the multiplicative approach, the PID control approach is smoother and has less oscillations.

6. RELATED WORK

6.1. Consistency-Latency Tradeoffs

In addition to the Weak CAP Principle [Fox and Brewer 1999] and PACELC [Abadi 2012] discussed in Section 1, there has been work on theoretically characterizing the tradeoff between latency and strong consistency models. Attiya and Welch [1994] studied the tradeoff between latency and linearizability and sequential consistency. Subsequent work has explored linearizability under different delay models [Eleftheriou and Mavronicolas 1999; Mavronicolas and Roth 1999]. All these papers are concerned with strong consistency models whereas we consider t -freshness, which models data freshness in eventually consistent systems. Moreover, their delay models are different from our partition model. There has been theoretical work on probabilistic quorum systems [Malkhi et al. 1997; Lee and Welch 2001; Abraham and Malkhi 2005]. Their consistency models are different from ours; moreover, they did not consider the tradeoff between consistency and availability.

There are two classes of systems that are closest to our work. The first class of systems are concerned with metrics for measuring data freshness or staleness. We do not compare our work against this class of systems in this paper, as it is not our goal to propose yet another consistency model

or metric. Bailis et al. [2013, 2014] proposed a probabilistic consistency model (PBS) for quorum-based stores, but did not consider latency, soft partitions or the CAP theorem. Golab et al. [2011] proposed a time-based staleness metric called Δ -atomicity. Δ -atomicity is considered the gold standard for measuring atomicity violations (staleness) across multiple read and write operations. The Γ metric [Golab et al. 2014] is inspired by the Δ metric and improves upon it on multiple fronts. For example, the Γ metric makes fewer technical assumptions than the Δ metric and produces less noisy results. It is also more robust against clock skew. All these related data freshness metrics cannot be directly compared to our t -freshness metric. The reason is that unlike our metric which considers write start times, these existing metrics consider end time of write operations when calculating data freshness.

The second class of systems deal with adaptive mechanisms for meeting consistency-latency SLAs for key-value stores. The Pileus system [Terry et al. 2013] considered families of consistency/latency SLAs, and requires the application to specify a utility value with each SLA. In comparison, PCAP considers probabilistic metrics of p_{ic}, p_{ua} . Tuba [Ardekani and Terry 2014] extended the predefined and static Pileus mechanisms with dynamic replica reconfiguration mechanisms to maximize Pileus style utility functions without impacting client read and write operations. Golab and Wylie [2014] proposed consistency amplification, which is a framework for supporting consistency SLAs by injecting delays at servers or clients. In comparison, in our PCAP system, we only add delays at servers. McKenzie et al. [2015] proposed continuous partial quorums (CPQ), which is a technique to randomly choose between multiple discrete consistency levels for fine-grained consistency-latency tuning, and compare CPQ against consistency amplification. Compared to all these systems where the goal is to meet SLAs, in our work, we also (1) quantitatively characterize the (un)achievable consistency-latency tradeoff envelope, and (2) show how to design systems that perform close to this envelope, in addition to (3) meeting SLAs. The PCAP system can be setup to work with any of these SLAs listed above; but we don't do this in the paper since our main goal is to measure how close the PCAP system is to the optimal consistency-latency envelope.

Recently, there has been work on declarative ways to specify application consistency and latency requirements – PCAP proposes mechanisms to satisfy such specifications [Sivaramakrishnan et al. 2015].

6.2. Adaptive Systems

There are a few existing systems that controls consistency in storage systems. FRACS [Zhang and Zhang 2003] controls consistency by allowing replicas to buffer updates up to a given staleness. AQuA [Krishnamurthy et al. 2003] continuously moves replicas between “strong” and “weak” consistency groups to implement different consistency levels. Fox and Brewer [1999] showed how to trade consistency (harvest) for availability (yield) in the context of the Inktomi search engine. While harvest and yield capture continuously changing consistency and availability conditions, we characterize the consistency-availability (latency) tradeoff in a quantitative manner. TACT [Yu and Vahdat 2002] controls staleness by limiting the number of outstanding writes at replicas (order error) and bounding write propagation delay (staleness). All the mentioned systems provide *best-effort* behavior for consistency, within the latency bounds. In comparison, the PCAP system explicitly allows applications to specify SLAs. Consistency levels have been adaptively changed to deal with node failures and network changes in [Davidson et al. 2013], however this may be intrusive for applications that explicitly set consistency levels for operations. Artificially delaying read operations at servers (similar to our read delay knob) has been used to eliminate staleness spikes (improve consistency) which are correlated with garbage collection in a specific key-value store (Apache Cassandra) [Fan et al. 2015]. Similar techniques have been used to guarantee causal consistency for client-side applications [Zawirski et al. 2015]. Simba [Perkins et al. 2015] proposed new consistency abstractions for mobile application data synchronization services, and allows applications to choose among various consistency models.

For stream processing, Gedik. et al. [2014] proposed a control algorithm to compute the optimal resource requirements to meet throughput requirements. There has been work on adaptive

elasticity control for storage [Lim et al. 2010], and adaptively tuning Hadoop clusters to meet SLAs [Herodotou et al. 2011]. Compared to the controllers present in these systems, our PCAP controller achieves control objectives [Hellerstein et al. 2004] using a different set of techniques to meet SLAs for key-value stores.

6.3. Composition

Composing local policies to form global policies is well studied in other domains, for example QoS composition in multimedia networks [Liang and Nahrstedt 2006], software defined network (sdn) composition [Monsanto et al. 2013], and web-service orchestration [Dustdar and Schreiner 2005]. Our composition techniques are aimed at consistency and latency guarantees for geo-distributed systems.

7. SUMMARY

In this paper, we have first formulated and proved a probabilistic variation of the CAP theorem which took into account probabilistic models for consistency, latency, and soft partitions within a data-center. Our theorems show the un-achievable envelope, i.e., which combinations of these three models make them impossible to achieve together. We then showed how to design systems (called PCAP) that (1) perform close to this optimal envelope, and (2) can meet consistency and latency SLAs derived from the corresponding models. We then incorporated these SLAs into Apache Cassandra and Riak running in a single data-center. We also extended our PCAP system from a single data-center to multiple geo-distributed data-centers. Our experiments with YCSB workloads and realistic traffic demonstrated that our PCAP system meets the SLAs, that its performance is close to the optimal-achievable consistency-availability envelope, and that it scales well. Simulations of our GeoPCAP system also showed SLA satisfaction for applications spanning multiple data-centers.

REFERENCES

- Daniel Abadi. 2012. Consistency Tradeoffs in Modern Distributed Database System Design: CAP is Only Part of the Story. *IEEE Computer* 45, 2 (2012), 37–42.
- Ittai Abraham and Dahlia Malkhi. 2005. Probabilistic quorums for dynamic systems. *Distributed Computing* 18, 2 (2005), 113–124.
- Masoud Saeida Ardekani and Douglas B. Terry. 2014. A Self-configurable Geo-replicated Cloud Storage System. In *Proceedings of the 11th USENIX Conference on Operating Systems Design and Implementation (OSDI)*. Broomfield, CO, USA, 367–381.
- K. J. Astrom and T. Hagglund. 1995. *PID Controllers: Theory, Design, and Tuning, 2nd Ed.* The Instrument, Systems, and Automation Society, Research Triangle Park, NC.
- Hagit Attiya and Jennifer L. Welch. 1994. Sequential Consistency Versus Linearizability. *ACM Transactions on Computer Systems (TOCS)* 12, 2 (1994), 91–122.
- Peter Bailis and Ali Ghodsi. 2013. Eventual Consistency Today: Limitations, Extensions, and Beyond. *ACM Queue* 11, 3 (2013), 20:20–20:32.
- Peter Bailis, Shivaram Venkataraman, Michael J. Franklin, JosephM. Hellerstein, and Ion Stoica. 2014. Quantifying eventual consistency with PBS. *The Very Large Data Bases (VLDB) Journal* 23, 2 (2014), 279–302.
- Peter Bailis, Shivaram Venkataraman, Michael J. Franklin, Joseph M. Hellerstein, and Ion Stoica. 2013. PBS at Work: Advancing Data Management with Consistency Metrics. In *Proceedings of the 2013 ACM SIGMOD International Conference on Management of Data (SIGMOD)*. New York, New York, USA, 1113–1116.
- R. Baldoni, C. Marchetti, and A. Virgillito. 2006. Impact of WAN Channel Behavior on End-to-end Latency of Replication Protocols. In *Proceedings of European Dependable Computing Conference (EDCC)*. Coimbra, Portugal, 109–118.
- Jeff Barr. 2013. Real-time ad impression bids using DynamoDB. <http://goo.gl/C7gdpc>.

- Theophilus Benson, Aditya Akella, and David A. Maltz. 2010. Network Traffic Characteristics of Datacenters in the Wild. In *Proceedings of the 10th ACM SIGCOMM Conference on Internet Measurement (IMC)*. Melbourne, Australia, 267–280.
- Eric Brewer. 2000. Towards robust distributed systems (Abstract). In *Proceedings of the Nineteenth Annual ACM Symposium on Principles of Distributed Computing (PODC)*. Portland, Oregon, USA.
- Eric Brewer. 2010. A Certain Freedom: Thoughts on the CAP Theorem. In *Proceedings of the 29th ACM SIGACT-SIGOPS Symposium on Principles of Distributed Computing (PODC)*. Zurich, Switzerland, 335–335.
- Adrian Cockcroft. 2013. Dystopia as a Service (Invited Talk). In *Proceedings of the 4th Annual Symposium on Cloud Computing (SoCC)*. Santa Clara, California.
- Brian F. Cooper, Adam Silberstein, Erwin Tam, Raghu Ramakrishnan, and Russell Sears. 2010a. Benchmarking cloud serving systems with YCSB. In *Proceedings of the 1st ACM Symposium on Cloud Computing (SoCC)*. Indianapolis, Indiana, USA, 143–154.
- Brian F. Cooper, Adam Silberstein, Erwin Tam, Raghu Ramakrishnan, and Russell Sears. 2010b. Yahoo! Cloud Serving Benchmark (YCSB). <http://goo.gl/GiA5c>.
- Brian F. Cooper, Adam Silberstein, Erwin Tam, Raghu Ramakrishnan, and Russell Sears. 2010c. Yahoo! Cloud Serving Benchmark (YCSB) Workloads. <https://github.com/brianfrankcooper/YCSB/wiki/Core-Workloads>.
- James C. Corbett, Jeffrey Dean, Michael Epstein, Andrew Fikes, Christopher Frost, J. J. Furman, Sanjay Ghemawat, Andrey Gubarev, Christopher Heiser, Peter Hochschild, Wilson Hsieh, Sebastian Kanthak, Eugene Kogan, Hongyi Li, Alexander Lloyd, Sergey Melnik, David Mwaura, David Nagle, Sean Quinlan, Rajesh Rao, Lindsay Rolig, Yasushi Saito, Michal Szymaniak, Christopher Taylor, Ruth Wang, and Dale Woodford. 2012. Spanner: Google’s Globally-distributed Database. In *Proceedings of the 10th USENIX Conference on Operating Systems Design and Implementation (OSDI)*. Hollywood, CA, USA, 251–264.
- DataStax. 2016. Configuring Data Consistency. <https://goo.gl/PKNUXV>
- Aaron Davidson, Aviad Rubinstein, Anirudh Todi, Peter Bailis, and Shivaram Venkataraman. 2013. Adaptive Hybrid Quorums in Practical Settings. <http://goo.gl/LbRSW3>.
- Jeff Dean. 2009. Design, Lessons and Advice from Building Large Distributed Systems. (2009). <http://goo.gl/HGJqUh>.
- Giuseppe DeCandia, Deniz Hastorun, Madan Jampani, Gunavardhan Kakulapati, Avinash Lakshman, Alex Pilchin, Swaminathan Sivasubramanian, Peter Vosshall, and Werner Vogels. 2007. Dynamo: Amazon’s Highly Available Key-value Store. In *Proceedings of Twenty-first ACM SIGOPS Symposium on Operating Systems Principles (SOSP)*. Stevenson, Washington, USA, 205–220.
- Schahram Dustdar and Wolfgang Schreiner. 2005. A Survey on Web Services Composition. *International Journal of Web and Grid Services* 1, 1 (2005), 1–30.
- Maria Eleftheriou and Marios Mavronicolas. 1999. Linearizability in the Presence of Drifting Clocks and Under Different Delay Assumptions. In *Distributed Computing*. Vol. 1693. 327–341.
- Hua Fan, Aditya Ramaraju, Marlon McKenzie, Wojciech Golab, and Bernard Wong. 2015. Understanding the Causes of Consistency Anomalies in Apache Cassandra. *Proceedings of the Very Large Data Bases (VLDB) Endowment* 8, 7 (2015), 810–813.
- Armando Fox and Eric A. Brewer. 1999. Harvest, Yield, and Scalable Tolerant Systems. In *Proceedings of the The Seventh Workshop on Hot Topics in Operating Systems (HotOS)*. Rio Rico, Arizona, USA, 174–178.
- Bugra Gedik., Scott Schneider, Martin Hirzel, and Kun-Lung Wu. 2014. Elastic Scaling for Data Stream Processing. *IEEE Transactions on Parallel and Distributed Systems (TPDS)* 25, 6 (2014), 1447–1463.
- Seth Gilbert and Nancy Lynch. 2002. Brewer’s Conjecture and the Feasibility of Consistent, Available, Partition-tolerant Web Services. *ACM SIGACT News* 33, 2 (2002), 51–59.
- Seth Gilbert and Nancy Lynch. 2012. Perspectives on the CAP Theorem. *IEEE Computer* 45, 2 (2012), 30–36.

- Eric Gilmore. 2011. Cassandra Multi data-center deployment. <http://goo.gl/aA8YIS>.
- Lisa Glendenning, Ivan Beschastnikh, Arvind Krishnamurthy, and Thomas Anderson. 2011. Scalable Consistency in Scatter. In *Proceedings of the Twenty-Third ACM Symposium on Operating Systems Principles (SOSP)*. Cascais, Portugal, 15–28.
- Wojciech Golab, Xiaozhou Li, and Mehul A. Shah. 2011. Analyzing consistency properties for fun and profit. In *Proceedings of the 30th Annual ACM SIGACT-SIGOPS Symposium on Principles of Distributed Computing (PODC)*. San Jose, California, USA, 197–206.
- Wojciech Golab, Muntasir Raihan Rahman, Alvin AuYoung, Kimberly Keeton, and Indranil Gupta. 2014. Client-Centric Benchmarking of Eventual Consistency for Cloud Storage Systems. In *Proceedings of the 2014 IEEE 34th International Conference on Distributed Computing Systems (ICDCS)*. Madrid, Spain.
- Wojciech Golab and John Johnson Wylie. 2014. Providing A Measure Representing an Instantaneous Data Consistency Level. (Jan. 2014). US Patent Application 20,140,032,504.
- Andy Gross. 2009. Basho Riak. <http://basho.com/riak/>.
- Joseph L. Hellerstein, Yixin Diao, Sujay Parekh, and Dawn M. Tilbury. 2004. *Feedback Control of Computing Systems*. John Wiley & Sons.
- Herodotos Herodotou, Fei Dong, and Shivnath Babu. 2011. No One (Cluster) Size Fits All: Automatic Cluster Sizing for Data-intensive Analytics. In *Proceedings of the 2nd ACM Symposium on Cloud Computing (SoCC)*. Cascais, Portugal, 18:1–18:14.
- Sudha Krishnamurthy, William H. Sanders, and Michel Cukier. 2003. An Adaptive Quality of Service Aware Middleware for Replicated Services. *IEEE Transactions on Parallel and Distributed Systems (TPDS)* 14 (2003), 1112–1125.
- Avinash Lakshman and Prashant Malik. 2008. Apache Cassandra. <http://cassandra.apache.org/>.
- Keith Lang. 2009. Amazon: milliseconds means money. <http://goo.gl/fs9pZb>.
- Hyunyoung Lee and Jennifer L. Welch. 2001. Applications of Probabilistic Quorums to Iterative Algorithms. In *Proceedings of the The 21st International Conference on Distributed Computing Systems (ICDCS)*. Phoenix (Mesa), Arizona, USA, 21.
- Cheng Li, Daniel Porto, Allen Clement, Johannes Gehrke, Nuno Preguica, and Rodrigo Rodrigues. 2012. Making Geo-replicated Systems Fast As Possible, Consistent when Necessary. In *Proceedings of the 10th USENIX Conference on Operating Systems Design and Implementation (OSDI)*. Hollywood, CA, USA, 265–278.
- Jin Liang and Klara Nahrstedt. 2006. Service Composition for Generic Service Graphs. *Multimedia Systems* 11, 6 (2006), 568–581.
- Harold C. Lim, Shivnath Babu, and Jeffrey S. Chase. 2010. Automated Control for Elastic Storage. In *Proceedings of the 7th International Conference on Autonomic Computing (ICAC)*. Washington, DC, USA, 1–10.
- LinkedIn. 2009. Project Voldemort. <http://goo.gl/9uhLoU>
- Wyatt Lloyd, Michael J. Freedman, Michael Kaminsky, and David G. Andersen. 2011. Don't Settle for Eventual: Scalable Causal Consistency for Wide-Area Storage with COPS. In *Proceedings of the Twenty-Third ACM Symposium on Operating Systems Principles (SOSP)*. Cascais, Portugal, 401–416.
- Wyatt Lloyd, Michael J. Freedman, Michael Kaminsky, and David G. Andersen. 2013. Stronger Semantics for Low-Latency Geo-Replicated Storage. In *Proceedings of the 10th USENIX Conference on Networked Systems Design and Implementation (NSDI)*. Lombard, IL, USA, 313–328.
- Dahlia Malkhi, Michael Reiter, and Rebecca Wright. 1997. Probabilistic Quorum Systems. In *Proceedings of the Sixteenth Annual ACM Symposium on Principles of Distributed Computing (PODC)*. Santa Barbara, California, USA, 267–273.
- Marios Mavronicolas and Dan Roth. 1999. Linearizable Read/Write Objects. *Theoretical Computer Science* 220, 1 (1999), 267 – 319.
- Marlon McKenzie, Hua Fan, and Wojciech Golab. 2015. Fine-tuning the Consistency-latency Trade-off in Quorum-replicated Distributed Storage Systems. In *Proceedings of the 2015 IEEE International Conference on Big Data*. Santa Clara, CA, USA, 1708–1717.

- Christopher Monsanto, Joshua Reich, Nate Foster, Jennifer Rexford, and David Walker. 2013. Composing Software-defined Networks. In *Proceedings of the 10th USENIX Conference on Networked Systems Design and Implementation (NSDI)*. Lombard, IL, USA, 1–14.
- Ron Peled. 2010. Activo: “Why Low Latency Matters?”. <http://goo.gl/2XQ8U1>
- Dorian Perkins, Nitin Agrawal, Akshat Aranya, Curtis Yu, Younghwan Go, Harsha V. Madhyastha, and Cristian Ungureanu. 2015. Simba: Tunable End-to-end Data Consistency for Mobile Apps. In *Proceedings of the Tenth European Conference on Computer Systems (EuroSys)*. Bordeaux, France, 7:1–7:16.
- Marc Shapiro. 1986. Structure and Encapsulation in Distributed Systems: the Proxy Principle. In *Proc. International Conference on Distributed Computing Systems (ICDCS)*. Cambridge, MA, USA, 198–204.
- Marc Shapiro, Nuno M. Prego, Carlos Baquero, and Marek Zawirski. 2011. Conflict-Free Replicated Data Types. In *Proceedings of the 13th International Conference on Stabilization, Safety, and Security of Distributed Systems (SSS)*. Grenoble, France, 386–400.
- K. C. Sivaramakrishnan, Gowtham Kaki, and Suresh Jagannathan. 2015. Declarative Programming Over Eventually Consistent Data Stores. In *Proceedings of the 36th ACM SIGPLAN Conference on Programming Language Design and Implementation (PLDI)*. Portland, OR, USA, 413–424.
- Ion Stoica, Robert Morris, David Karger, M. Frans Kaashoek, and Hari Balakrishnan. 2001. Chord: A Scalable Peer-to-peer Lookup Service for Internet Applications. In *Proceedings of the 2001 Conference on Applications, Technologies, Architectures, and Protocols for Computer Communications (SIGCOMM)*. San Diego, California, USA, 149–160.
- Shlomo Swidler. 2009. Consistency in Amazon S3. <http://goo.gl/yhAoJy>.
- Douglas B. Terry, Vijayan Prabhakaran, Ramakrishna Kotla, Mahesh Balakrishnan, Marcos K. Aguilera, and Hussam Abu-Libdeh. 2013. Consistency-based Service Level Agreements for Cloud Storage. In *Proceedings of the Twenty-Fourth ACM Symposium on Operating Systems Principles (SOSP)*. Farmington, Pennsylvania, USA, 309–324.
- Werner Vogels. 2009. Eventually Consistent. *Communications of the ACM (CACM)* (2009), 40–44.
- Hengfeng Wei, Yu Huang, Jiannong Cao, and Jian Lu. 2015. Almost Strong Consistency: “Good Enough” in Distributed Storage Systems. <http://arxiv.org/abs/1507.01663>.
- Brian White, Jay Lepreau, Leigh Stoller, Robert Ricci, Shashi Guruprasad, Mac Newbold, Mike Hibler, Chad Barb, and Abhijeet Joglekar. 2002. An Integrated Experimental Environment for Distributed Systems and Networks. In *Proceedings of the Fifth Symposium on Operating Systems Design and Implementation (OSDI)*. Boston, Massachusetts, 255–270.
- Haifeng Yu and Amin Vahdat. 2002. Design and Evaluation of a Conit-based Continuous Consistency Model for Replicated Services. *ACM Transactions on Computer Systems (TOCS)* 20, 3 (2002), 239–282.
- Marek Zawirski, Nuno Prego, Sérgio Duarte, Annette Bieniusa, Valter Bolegás, and Marc Shapiro. 2015. Write Fast, Read in the Past: Causal Consistency for Client-Side Applications. In *Proceedings of the 16th Annual Middleware Conference*. Vancouver, BC, Canada, 75–87.
- Chi Zhang and Zheng Zhang. 2003. Trading Replication Consistency for Performance and Availability: an Adaptive Approach. In *Proceedings of the 23rd International Conference on Distributed Computing Systems (ICDCS)*. Providence, Rhode Island, USA, 687–695.